Acta Neuropathologica (2019) 137:801–823
https://doi.org/10.1007/s00401-019-01967-4

ORIGINAL PAPER

Beta-amyloid pathology in human brain microvessel extracts from the parietal cortex: relation with cerebral amyloid angiopathy and Alzheimer's disease

Philippe Bourassa[1,2] · Cyntia Tremblay[2] · Julie A. Schneider[3] · David A. Bennett[3] · Frédéric Calon[1,2]

Received: 14 September 2018 / Revised: 24 January 2019 / Accepted: 24 January 2019 / Published online: 7 February 2019

Abstract

Several pieces of evidence suggest that blood–brain barrier (BBB) dysfunction is implicated in the pathophysiology of Alzheimer's disease (AD), exemplified by the frequent occurrence of cerebral amyloid angiopathy (CAA) and the defective clearance of Aβ peptides. However, the specific role of brain microvascular cells in these anomalies remains elusive. In this study, we validated by Western, ELISA and immunofluorescence analyses a procedure to generate microvasculature-enriched fractions from frozen samples of human cerebral cortex. We then investigated Aβ and proteins involved in its clearance or production in microvessel extracts generated from the parietal cortex of 60 volunteers in the Religious Orders Study. Volunteers were categorized as AD ($n=38$) or controls ($n=22$) based on the ABC scoring method presented in the revised guidelines for the neuropathological diagnosis of AD. Higher ELISA-determined concentrations of vascular Aβ40 and Aβ42 were found in persons with a neuropathological diagnosis of AD, in apoE4 carriers and in participants with advanced parenchymal CAA, compared to respective age-matched controls. Vascular levels of two proteins involved in Aβ clearance, ABCB1 and neprilysin, were lower in persons with AD and positively correlated with cognitive function, while being inversely correlated to vascular Aβ40. In contrast, BACE1, a protein necessary for Aβ production, was increased in individuals with AD and in apoE4 carriers, negatively correlated to cognitive function and positively correlated to Aβ40 in microvessel extracts. The present report indicates that concentrating microvessels from frozen human brain samples facilitates the quantitative biochemical analysis of cerebrovascular dysfunction in CNS disorders. Data generated overall show that microvessels extracted from individuals with parenchymal CAA–AD contained more Aβ and BACE1 and less ABCB1 and neprilysin, evidencing a pattern of dysfunction in brain microvascular cells contributing to CAA and AD pathology and symptoms.

Keywords Blood–brain barrier · Brain microvascular cells · Alzheimer's disease · Cerebral amyloid angiopathy · Beta-amyloid

Introduction

Alzheimer's disease (AD) is the leading cause of dementia, affecting over 40 million people worldwide. From a neuropathological standpoint, AD is characterized by an extracellular accumulation of beta-amyloid peptides (Aβ) forming plaques, intracellular accumulation of hyperphosphorylated tau, and degeneration of neurons and synapses [88, 89]. However, despite decades of research, the exact pathophysiological cause of AD has yet to be identified.

Evidence of vascular pathology in the development of AD has been collected for many years [53, 60]. For instance, thickening of the basal membrane and reduced microvessel density have been repeatedly reported in postmortem AD brains [22, 35, 59, 86, 110]. Functional changes have also

Electronic supplementary material The online version of this article (https://doi.org/10.1007/s00401-019-01967-4) contains supplementary material, which is available to authorized users.

✉ Frédéric Calon
Frederic.Calon@crchul.ulaval.ca

[1] Faculté de pharmacie, Université Laval, Quebec, QC, Canada

[2] Axe Neurosciences, Centre de recherche du CHU de Québec-Université Laval, 2705, Boulevard Laurier, Room T2-67, Quebec, QC G1V 4G2, Canada

[3] Rush Alzheimer's Disease Center, Rush University Medical Center, Chicago, IL, USA

been described, including decreased glucose uptake and cerebral blood flow in AD patients compared to controls [45, 50, 75]. Beside their extracellular accumulation in neuritic plaques, the accumulation of Aβ in vessel walls, which is termed cerebral amyloid angiopathy (CAA) [17, 77], is frequently observed in the cortex while rarely seen in deep brain regions and absent in white matter [95]. Two types of CAA have been reported, i.e., CAA type 1 when Aβ deposits are found in leptomeningeal and cortical arteries, arterioles, veins and venules, as well as capillaries; and CAA type 2 when leptomeningeal and cortical vessels, except capillaries, are affected [83]. CAA is very common in persons with AD, with proportions, regardless of severity, ranging from 55% to virtually 100%, depending on the study [7, 53, 54, 74, 82, 106]. The extent of CAA, determined by immunological detection of Aβ or Congo Red staining on brain sections and quantified either as a continuous severity score or the number of Aβ-laden microvessels, was also shown to be correlated to cognitive decline [7, 53] or other hallmark pathological features of AD [9, 107]. Other sets of reports indicate that apolipoprotein E4 (apoE4) carriage increases the risk of developing CAA [24, 74, 82], possibly through enhancing deposition of Aβ40, but not Aβ42 [62].

The hypothesis that brain endothelial cells forming the blood–brain barrier (BBB) become dysfunctional in AD is currently gaining support [10, 34, 112]. Accumulated data suggest that brain-to-blood Aβ clearance is reduced in AD [65], which could be explained by a shift toward more influx (receptor for advanced glycation end products/RAGE) and less efflux (low-density lipoprotein receptor-related protein 1/LRP1 and ABCB1/*P*-glycoprotein) transporters and receptors at the BBB [32, 66, 79, 102], although it has also been reported that RAGE and LRP1 were not altered in AD compared to controls [103]. Neprilysin, a major Aβ-degrading enzyme in the brain [100], is also found in the cerebral vasculature [23] and experiments on brain sections revealed that neprilysin levels in microvessels of the frontal cortex were reduced in AD compared to controls [68]. Finally, although most of the cerebral Aβ is produced by neurons, brain microvascular endothelial cells were also shown to harbor amyloid precursor protein (APP) and β-secretase (BACE1) and may thus be directly involved in Aβ production locally [30, 105]. In light of these reports, brain microvascular cells have the enzymes and transporters/receptors to alter the clearance and production of Aβ. Nevertheless, the extent by which they contribute to the accumulation of Aβ in brain vasculature and how their dysfunction is associated with the development of CAA and AD remain undefined.

Most of the postmortem data gathered so far on vascular pathology and BBB dysfunction in AD have come from histological staining or immunological detection on brain sections. For instance, CAA, Aβ and its BBB transporters and receptors, as well as Aβ-degrading enzymes and key players in the amyloidogenic pathway have rarely been studied directly in cerebral microvessels by techniques other than immunohistochemistry or immunofluorescence, which offer limited possibilities for size- or solubility-based separation and quantification. It has been proposed that methods using isolated cerebral microvessels could provide better estimates of the true prevalence and distribution of CAA in AD or at least give a different perspective on the role of CAA in the etiology of AD [101]. Hence, we established, based on previously published methodologies using fresh tissue [2, 18, 109], a method to generate a fraction enriched in microvessels from frozen human brain samples. We used parietal cortex samples from participants in the Religious Orders Study who underwent detailed clinical and neuropsychological evaluation [1, 14]. In this study, we focused on the analysis of Aβ concentrations, BBB transporters and receptors putatively involved in Aβ transport, neprilysin and key players in Aβ production to improve our comprehension on the role of brain microvascular cells regarding Aβ clearance and production in the pathogenesis of CAA and AD.

Methods

Human samples: Religious Orders Study (Rush Alzheimer's Disease Center)

Inferior parietal cortex samples were obtained from participants in the Religious Orders Study, a longitudinal clinical and pathological cohort study of aging and dementia from which extensive amounts of clinical and neuropathological data were available [1, 11, 14]. Each participant enrolled without known dementia and underwent uniform structured clinical evaluations until death. Briefly, dementia and AD diagnosis required evidence of meaningful decline in cognitive function and impairment in at least two domains of cognition, one of which was episodic memory, based on the results of 21 cognitive performance tests and their review by a clinical neuropsychologist and expert clinician [12]. "MCI" refers to participants with cognitive impairment as assessed by the neuropsychologist but without a diagnosis of dementia, as determined by the clinician [16]. A global measure of cognition along with five cognitive domains (episodic, semantic and working memory, perceptual speed and visual-spatial ability) was generated from 19 cognitive performance tests [104]. Each participant was also interviewed about their current prescription medication usage, such as antihypertensive and diabetes medications, in the last 2 weeks prior to follow-up as reported [5, 8]. At death, a neurologist, blinded to all pathologic data, reviewed select clinical data and rendered a summary diagnostic opinion regarding the clinical diagnosis at the time of death. Participants thus received

a clinical diagnosis of MCI ($n = 20$) or AD ($n = 20$), and persons with no cognitive impairment were classified as NCI ($n = 20$), as previously described [13]. The neuropathological assessment was performed using the ABC scoring method found in the revised National Institute of Aging-Alzheimer's Association (NIA-AA) guidelines for the neuropathological diagnosis of AD [70]. Each case was given, by examiners blinded to all clinical data [15], an ABC score integrating the scores obtained from the evaluation of three different parameters: (A) Thal score assessing phases of Aβ plaque accumulation [85], (B) Braak score assessing neurofibrillary tangle pathology [20], and (C) CERAD score assessing neuritic plaque pathology [69]. ABC scores were reported as AX, BX, CX with X ranging from 0 to 3 for each parameter [70]. Neuritic plaques, diffuse plaques, and neurofibrillary tangles in the parietal cortex were counted following Bielschowsky silver impregnation, as previously described. Using the chart described in the revised NIA-AA guidelines, each ABC score was converted into one of four levels of AD neuropathological changes: not, low, intermediate or high. According to this chart, intermediate or high levels of AD neuropathological changes are consistent with a neuropathological diagnosis of AD, while no or a low level of AD neuropathological changes are not [70]. Therefore, in this study, individuals with intermediate or high levels of AD neuropathological changes were pooled together as the AD group, while participants with no or a low level of AD neuropathological changes were pooled together as the control group. In addition, the presence of cerebral macroinfarcts and microinfarcts was determined during neuropathological evaluations and coded as a binary scale as following: 0, no infarcts; 1, one or more infarcts, as described previously [6]. Table 1 summarizes clinical, neuropathological and biochemical data of participants grouped by the level of AD neuropathological changes.

Cerebral amyloid angiopathy staging

CAA staging of parenchymal vessels in the parietal cortex was performed as previously described [19]. Briefly, paraffin-embedded sections from the angular gyrus were immunostained for β-amyloid using one of three monoclonal anti-human antibodies: 4G8 (1:9000; Covance Labs, Madison, WI), 6F/3D (1:50; Dako North America Inc., Carpinteria, CA), and 10D5 (1:600; Elan Pharmaceuticals, San Francisco, CA). Parenchymal vessels from the whole gyrus were evaluated for amyloid deposition and staged from 0 to 4, where 0 = no deposition, 1 = scattered segmental but no circumferential deposition, 2 = circumferential deposition up to 10 vessels, 3 = circumferential deposition up to 75% of the region, and 4 = circumferential deposition over 75% of the total region.

Preparation of whole brain homogenates

Each inferior parietal cortex sample (~ 100 mg) was sequentially centrifuged to generate a Tris-buffered saline (TBS)-soluble protein fraction containing soluble intracellular, nuclear and extracellular proteins, a detergent-soluble fraction containing membrane-bound proteins and a detergent-insoluble fraction containing insoluble aggregates, as previously shown [47, 48, 89]. The resulting whole homogenates of total soluble proteins were then used for comparison with microvessel-enriched extracts.

Isolation of human brain microvessels

The protocol used for microvessel enrichment, schematized in Fig. 1a, was designed for frozen human brain samples as starting material. It was adapted from our previous publications [2, 3, 31, 87], as well as from Yousif et al. [109] and from Boulay et al. [18]. We performed microvessel isolation in the parietal cortex as this brain region was shown to be affected early in the development of AD and to be plagued by neuropathological hallmarks of AD such as amyloid plaques, neurofibrillary tangles, synaptic protein deficiency and TDP43 aggregation [88–90], and CAA [84], making it particularly relevant for studying the relationship between CAA and AD. Separate inferior parietal cortex samples (~ 400 mg) were thawed on ice in 500 µl of a microvessel isolation buffer (MIB; 15 mM HEPES, 147 mM NaCl, 4 mM KCl, 3 mM $CaCl_2$ and 12 mM $MgCl_2$) containing a cocktail of protease and phosphatase inhibitors (Bimake, Houston, TX). Meninges and all visible white matter were removed with tweezers and samples were transferred in a 2 ml tissue grinder. Samples were then homogenized in a total of 1.5 ml of MIB, transferred in a 15 ml conical tube and centrifuged at 1000 *g* for 10 min at 4 °C. The supernatant was removed, the pellet was resuspended in 5 ml of MIB containing 18% dextran (from leuconostoc mesenteroides, M.W. 60,000–90,000; Sigma-Aldrich, St. Louis, MO) and spun at 4000 *g* for 20 min at 4 °C. The resulting supernatant was discarded to avoid contamination of the pellet by the myelin layer. Then, the tube was cleaned with absorbent paper and the pellet was resuspended in 1 ml of MIB. The homogenate was then filtered through a 20 µm nylon filter (Millipore, Temecula, CA). The material that was retained on the filter consists of cerebral microvessels, whereas the filtrate consists of microvessel-depleted parenchymal cell populations. The collected vascular tissue was washed off the filter with 500 µl of lysis buffer (150 mM NaCl, 10 mM NaH_2PO_4, 1% Triton X-100, 0.5% SDS and 0.5% sodium

Table 1 Cohort characteristics

Characteristics	Control	AD	Statistical analysis
N	22	38	–
Men, %	41	29	C; Pearson test, $\chi^2 = 0.897$; $p = 0.3436$
Mean age at death	86.7 (4.3)	87.5 (5.7)	Mann–Whitney test, $p = 0.5548$
Mean education, years	18.3 (3.5)	18.1 (3.1)	Mann–Whitney test, $p = 0.5236$
Mean MMSE	25.0 (4.5)	21.6 (7.9)	Mann–Whitney test, $p = 0.0791$
Global cognition score	− 0.32 (0.81)	− 0.94 (0.93)$^{\#}$	Mann–Whitney test, $p = 0.0044$
apoE ε4 allele carriage (%)	9	45$^{\$}$	C; Pearson test, $\chi^2 = 8.182$; $p = 0.0042$
Clinical diagnosis NCI/MCI/AD (*n*)	11/8/3	9/12/17	–
Thal amyloid score 0/1/2/3 (n)	7/13/2/0	0/3/15/20	–
Braak score 0/1/2/3 (n)	0/7/15/0	0/0/27/11	–
CERAD score 0/1/2/3 (n)	14/4/4/0	1/3/16/18	–
Parenchymal CAA stage in parietal cortex 0/1/2/3/4 (*n*)	15/4/1/1/0	18/7/5/2/3	C; Pearson test, $\chi^2 = 3.830$; $p = 0.4295$
Presence of chronic cortical macroinfarcts 0/1 (*n*)	20/2	33/5	C; Pearson test, $\chi^2 = 0.224$; $p = 0.6363$
Presence of chronic cortical microinfarcts 0/1 (*n*)	17/5	34/4	C; Pearson test, $\chi^2 = 1.627$; $p = 0.2021$
Usage of antihypertensive medication 0/1 (*n*)	2/20	5/33	C; Pearson test, $\chi^2 = 0.224$; $p = 0.6363$
Usage of diabetes medication 0/1 (*n*)	15/7	33/5	C; Pearson test, $\chi^2 = 3.032$; $p = 0.0816$
Cerebellar pH	6.39 (0.37)	6.29 (0.36)	Mann–Whitney test, $p = 0.2933$
Postmortem delay, h	7.93 (5.11)	7.53 (5.15)	Mann–Whitney test, $p = 0.6652$
Diffuse plaque counts in parietal cortex	3.8 (8.0)	20.3 (16.8)$^{\&}$	Mann–Whitney test, $p < 0.0001$
Neuritic plaque counts in parietal cortex	1.3 (3.2)	15.7 (12.5)$^{\&}$	Mann–Whitney test, $p < 0.0001$
Neurofibrillary tangle counts	0.09 (0.43)	2.92 (8.35)$^{\#}$	Mann–Whitney test, $p = 0.0096$
Soluble Aβ40 concentration, pmol/L	125.4 (245.9)	363.2 (695.2)¶	Mann–Whitney test, $p = 0.0009$
Soluble Aβ42 concentration, pmol/L	299.6 (475.0)	1173.6 (503.9)$^{\&}$	Mann–Whitney test, $p < 0.0001$
Soluble Aβ40/Aβ42 ratio	0.99 (1.09)	0.34 (0.59)	Mann–Whitney test, $p < 0.0001$
Cyclophilin B in microvessel extracts (loading control)	2.74 (0.77)	2.66 (0.79)	Mann–Whitney test, $p = 0.7309$
Claudin-5 levels in microvessel extracts (normalized ROD)	1.17 (0.50)	1.16 (0.41)	Mann–Whitney test, $p = 0.6613$
CD31 levels in microvessel extracts (normalized ROD)	0.45 (0.40)	0.41 (0.36)	Mann–Whitney test, $p = 0.7366$

Participants were assigned to the "Control" or "AD" group based on the level of AD neuropathological changes associated with their ABC scores [70]. ABC scores were converted into one of the four levels of AD neuropathological changes (not, low, intermediate or high) using the chart described in the revised NIA-AA guidelines [70]. Intermediate or high levels of AD neuropathological changes were assigned to the "AD" group, while those with no or a low level of AD neuropathological changes were rather assigned to the "Control" group [70]. Parenchymal CAA stages in the parietal cortex were determined in the angular gyrus. Brain pH was measured in cerebellum extracts. Soluble Aβ peptide concentrations were determined by ELISA in whole homogenates of inferior parietal cortex. Values are expressed as means (SD) unless specified otherwise. Statistical analysis (compared to controls): Mann–Whitney test, $^{\#}p < 0.01$; $^{¶}p < 0.001$; $^{\&}p < 0.0001$; Pearson test, $^{\$}p < 0.01$. Claudin-5 and CD31 data in microvessel extracts were normalized with cyclophilin B as loading control. *AD* Alzheimer's disease, *C* contingency, *CAA* cerebral amyloid angiopathy, *CERAD* Consortium to Establish a Registry for Alzheimer's Disease, *MCI* mild cognitive impairment, *NCI* healthy controls with no cognitive impairment, *ROD* relative optical density

deoxycholate) containing protease and phosphatase inhibitors and 1 mM EDTA. The microvessels were then homogenized and disrupted by sonication (3 × 45 s) in a Sonic Dismembrator apparatus (Thermo Fisher Scientific, Waltham, MA) and spun at 100,000*g* for 20 min at 4 °C. The resulting supernatant was concentrated by a centrifugation at 16,000*g* for 60 min at 4 °C in a Vivaspin device (MWCO, 3 kDa; Sartorius Stedim Biotech, Aubagne, France) and preserved for Western immunoblotting analyses as the vascular fraction. The pellet, containing the detergent-insoluble material, was homogenized in 125 µl of formic acid, sonicated and spun at 16,000 *g* for 20 min at 4 °C. Formic acid was evaporated from the resulting supernatant and the material was either resuspended in Laemmli's loading buffer (for Western blot analyses; not used in this study) or in a 5 M guanidium solution in Tris–HCl 50 mM (for ELISA analyses). In parallel, the filtrate was spun at 16,000 *g* for 20 min at 4 °C. The resulting pellet was homogenized in 100 µl of lysis buffer, sonicated and spun at 100,000 *g* for 20 min at 4 °C. The supernatant was preserved for Western immunoblotting analyses as the microvessel-depleted parenchymal fraction. Protein concentrations in all fractions were determined using the bicinchoninic acid assay (Thermo Fisher Scientific).

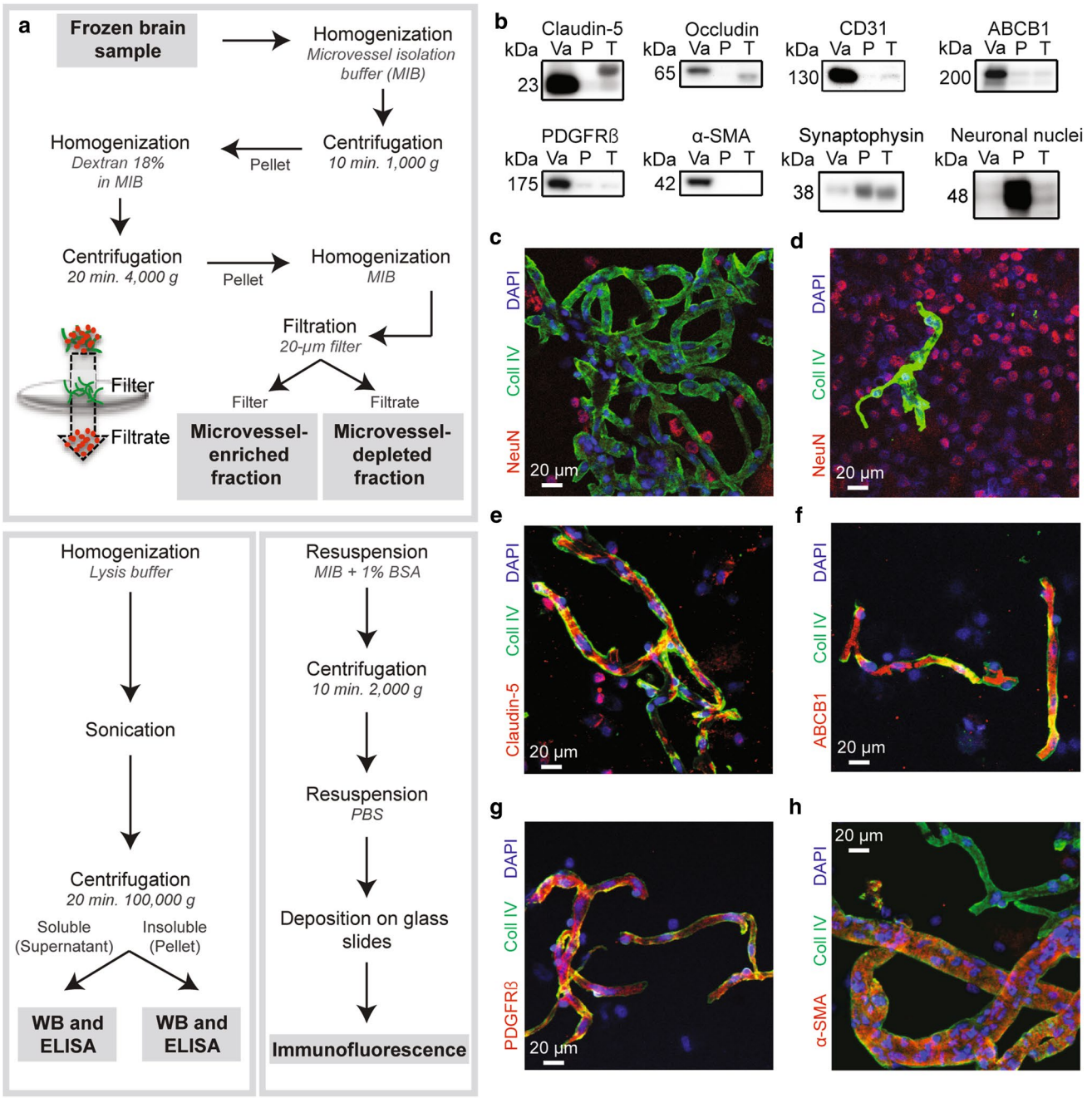

Fig. 1 Validation of the microvessel enrichment protocol. **a** Workflow leading to the separation of the microvessel-enriched and the microvessel-depleted parenchymal fractions, respectively, illustrated in green and red in the filtration scheme, from whole homogenates of cerebral cortex, and subsequent steps allowing for Western blot, ELISA and immunofluorescence experiments. **b** Microvessel extracts show enrichment in endothelial markers like claudin-5, occludin, CD31/PECAM and ABCB1/*P*-glycoprotein, and mural cell markers PDGFRβ and α-SMA, while synaptophysin and NeuN, both neuronal markers, are rather enriched in the microvessel-depleted parenchymal fraction. All samples were generated from frozen blocks of parietal cortices. Consecutive bands were taken for all representative photo examples. The same amount (8 µg) of proteins per sample was loaded. **c**–**f** Validation by immunofluorescence showed that microvessels, stained with type IV collagen, a marker of basal membrane (green), are concentrated in the vascular fraction (**c**) compared to the microvessel-depleted parenchymal fraction (**d**). On the contrary, immunostaining of neuronal nuclei (NeuN, red) in both fractions revealed that neurons are predominantly found in the microvessel-depleted parenchymal fraction (**d**). Type IV collagen-positive microvessels were also stained by claudin-5 (**e**), ABCB1 (**f**), PDGFRβ (**g**) and α-SMA (**h**) antibodies. Magnification used: 20 ×. Scale bar: 20 µm. *P* microvessel-depleted parenchymal fraction, *T* total homogenate, *Va* vascular fraction, enriched in microvessels, *WB* Western blot

Western blot

Proteins from human microvessel extracts or total soluble protein homogenates were added to Laemmli's loading buffer and heated 10 min at 70 °C. Equal amounts of proteins per sample (8 µg) were resolved on a sodium dodecyl sulfate–polyacrylamide gel electrophoresis (SDS–PAGE). Proteins were electroblotted on PVDF membranes, which were then blocked during 1 h at RT with a PBS solution containing 5% non-fat dry milk, 0.5% BSA and 0.1% Tween 20. Membranes were then incubated overnight at 4 °C with the primary antibodies listed in Table 2. Membranes were then washed three times with PBS containing 0.1% Tween 20 and incubated during 1 h at RT with the secondary antibody (goat anti-rabbit HRP, goat anti-mouse HRP or goat anti-rat HRP; Jackson ImmunoResearch Laboratories, West Grove, PA; 1:50,000 in PBS containing 0.1% Tween 20 and 1% BSA). Membranes were probed with chemiluminescence reagent (Luminata Forte Western HRP substrate; Millipore) and imaged using the myECL imager system (Thermo Fisher Scientific). Densitometric analysis was performed using the myImageAnalysis™ Software provided with the imaging system.

Immunofluorescence analysis of isolated microvessels

For immunofluorescence experiments, samples of vascular tissue collected from the filter after dextran separation were resuspended in 3 ml of MIB with 1% BSA and protease and phosphatase inhibitors and spun at 2000 *g* for 10 min at 4 °C. The supernatant was discarded and the pellet was resuspended in 100 µl of phosphate buffer saline (PBS). In parallel, the filtrate containing the microvessel-depleted parenchymal material was spun at 12,000 *g* for 5 min at 4 °C and the resulting pellet was resuspended in 200 µl of PBS. Vascular and microvessel-depleted extracts were then deposited on glass slides (5 µl per slide) and left at RT for 30 min to allow adhesion. Afterwards, both extracts were fixed using a 4% paraformaldehyde solution in PBS for 20 min at RT, washed three times with PBS and then blocked with a 10% normal horse serum (NHS) and 0.1% Triton X-100 solution in PBS for 1 h at RT. For Aβ immunolabeling only, a pretreatment with 90% formic acid during 10 min was performed between the fixation and blockage steps. Following an incubation overnight at 4 °C with primary antibodies (Table 2) diluted in a 1% NHS and 0.05% Triton X-100 solution in PBS, vascular and microvessel-depleted extracts were incubated with secondary antibodies (donkey anti-goat Alexa Fluor 488, donkey anti-mouse Alexa Fluor 647 or donkey anti-rabbit Alexa Fluor 647, all 1:500) diluted in the

Table 2 List of antibodies used in this study

Protein	Role/localization	Host	Dilution		Company	Catalog number
			WB	IF		
α-SMA	Smooth muscle cell	Rabbit	1:1000	1:100	Abcam	ab5694
Aβ40	Aβ peptide	Mouse	–	1:100	BioLegend	805401
Aβ42	Aβ peptide	Mouse	–	1:100	BioLegend	805501
ABCB1	BBB transporter	Rabbit	1:2000	1:100	Abcam	ab170904
APP	Aβ precursor	Mouse	1:500	–	BioLegend	803003
BACE1	Aβ production	Rabbit	1:500	–	Abcam	ab108394
CD31	EC intercellular junctions	Rabbit	1:1000	–	Abcam	ab28364
Claudin-5	EC intercellular junctions	Rabbit	1:2000	1:100	Santa Cruz Biotechnology	sc-28670; discontinued
Cyclophilin B	Loading control	Rabbit	1:1000	–	Abcam	ab16045
LRP1	BBB receptor	Rabbit	1:20000	–	Abcam	ab92544
Neprilysin	Aβ-degrading enzyme	Rabbit	1:2000	–	Abcam	ab79423
NeuN	Neuronal nuclei	Rabbit	1:1000	1:1000	Abcam	ab177487
Occludin	EC intercellular junctions	Rabbit	1:1000	–	Invitrogen	71-1500
PDGFRβ	Pericyte receptor	Rabbit	1:2000	1:100	Abcam	ab32570
RAGE	BBB receptor	Rat	1:2000	–	R&D Systems	MAB11795
Synaptophysin	Presynaptic vesicles	Mouse	1:20000	–	Millipore	MAB368; discontinued
Type IV collagen	Basal membrane	Goat	–	1:500	Millipore	AB769

Aβ beta-amyloid peptides, *ABCB1 P*-glycoprotein, *APP* amyloid protein precursor, *BACE1* β-secretase, *BBB* blood–brain barrier, *CD31* platelet endothelial cell adhesion molecule, *EC* endothelial cell, *IF* immunofluorescence, *LRP1* low-density lipoprotein receptor-related protein 1, *NeuN* neuronal nuclei, *RAGE* receptor for advanced glycation end products, *WB* Western blot

same solution as the primary antibodies during 1 h at RT. Cell nuclei were counterstained with DAPI (Thermo Fisher Scientific, 0.02% in PBS) and slides were mounted with Mowiol mounting medium. Between each step, three washes of 5 min in PBS were performed. Incubations were all performed in a humid chamber. Images were taken using a confocal laser scanning microscope (Olympus IX81-FV1000; Ontario, Canada) and were acquired by sequential scanning using optimal z-separation at a magnification of 20 ×.

Elisa

Aβ40 and Aβ42 concentrations in TBS-soluble protein fractions from whole homogenates and both detergent-soluble and detergent-insoluble fractions obtained from brain microvessel extracts were determined using highly sensitive ELISA kits according to the manufacturer's instructions (Wako, Osaka, Japan), as previously described [88, 89].

Data and statistical analysis

When comparing two groups, the normality of data distribution within each group was assessed using the Shapiro–Wilk test. If the data distribution of either one or both groups failed to pass the normality test, groups were compared using a non-parametric Mann–Whitney test. Otherwise, an unpaired Student's *t* test was performed. When more than two groups were compared, non-parametric Kruskal–Wallis ANOVA followed by Dunn's multiple comparison tests or two-way ANOVA were used. Correlations with antemortem clinical scores were adjusted for the following covariates: gender, age at death, educational level and *APOE* genotype. For all data, statistical significance was set at $p < 0.05$. Individual data were excluded for technical reasons or if determined as an outlier. All statistical analyses were performed with Prism 6 (GraphPad, San Diego, CA, USA) or JMP (version 13; SAS Institute Inc., Cary, IL) softwares.

Results

Generation of a vasculature-enriched fraction from frozen human brain tissue

The vascular enrichment procedure we used in this study is schematically represented in Fig. 1a. Given that we started with frozen human brain samples as compared to fresh brain samples in previous studies, we first validated that microvessels were efficiently enriched using this type of processing. Various endothelial, mural and non-endothelial markers were probed using both Western blot and immunofluorescence, with antibodies described in Table 2. As shown in Fig. 1b, endothelial markers claudin-5, occludin, CD31/PECAM and ABCB1/*P*-glycoprotein were greatly enriched in the vascular fraction. Platelet-derived growth factor receptor β (PDGFRβ) and alpha smooth muscle actin (α-SMA), the respective markers of pericytes and smooth muscle cells, were also concentrated in the vascular fraction. Conversely, synaptophysin and neuronal nuclei (NeuN), antigens exclusively expressed in neurons, were predominantly found in the microvessel-depleted fraction. Densitometry analysis revealed that all the endothelial markers selected were enriched at least eightfold in the vascular fraction, demonstrating that the method used successfully concentrated brain microvessels, compared to the microvessel-depleted fraction containing the rest of the parenchyma. To extend our validation using immunofluorescence experiments, we exposed both fractions to type IV collagen and NeuN antibodies as markers of microvessels and neurons, respectively (Fig. 1c, d). We observed an abundant type IV collagen staining and scarce NeuN-positive cells in the vascular fraction (Fig. 1c). In sharp contrast, NeuN-positive cells heavily outnumbered type IV collagen-positive capillaries in microvessel-depleted filtrates (Fig. 1d). Type IV collagen-positive microvessels were also positive for claudin-5 (Fig. 1e), ABCB1/*P*-glycoprotein (Fig. 1f), PDGFRβ (Fig. 1g), and α-SMA (Fig. 1h). Altogether, these observations indicate that capillaries, as well as larger vessels like arterioles and arteries, were concentrated using our method, retaining expression of endothelial and mural markers. Since we did not use markers to discriminate venules and veins, we cannot rule out their presence, given that their diameter is similar to that of arterioles. Throughout this study, the term "microvessel" refers to all vessel types found in our vascular extracts.

Parenchymal microvessel CAA in the parietal cortex

Since Aβ40 peptides have been previously reported to accumulate preferentially in the cerebrovasculature [49], we also investigated the proportion of Aβ40 and Aβ42 in vascular extracts from the 60 individuals included in this study. As presented in Fig. 2a, ratios of soluble Aβ40/Aβ42 from microvessel extracts were approximately threefold higher compared to whole homogenates from the same parietal cortex samples (1.5 versus 0.5), confirming the tendency of Aβ40 to be more abundant than Aβ42 in microvessels. Furthermore, qualitative evaluation of parenchymal microvessel CAA by immunostaining confirmed previously described CAA staging. Indeed, a clear signal highlighting amyloid accumulation was seen in larger vessels of the parietal cortex at stage 4 CAA (Fig. 2b, c), whereas no immunoreactivity for Aβ was detected at stage 0 CAA (Aß42 shown in Fig. 2d). No signal was found in smaller vessels.

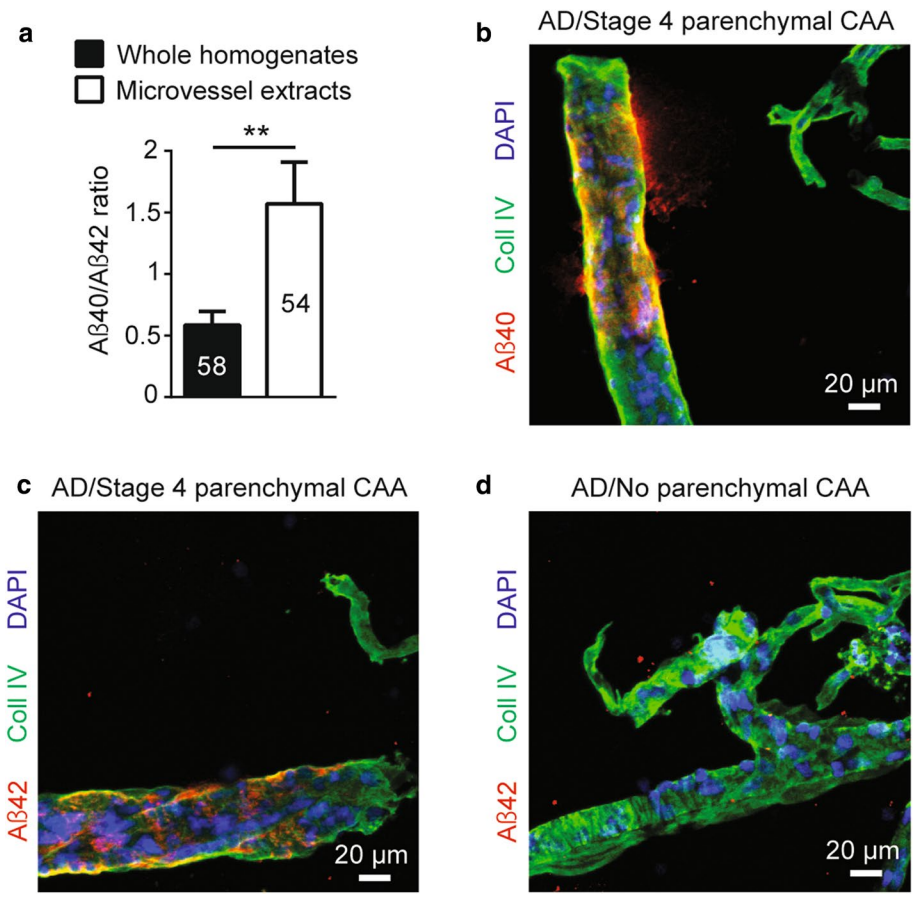

Fig. 2 Localization of Aβ peptides in microvessel extracts from the parietal cortex. **a** Concentrations of Aβ40, Aβ42 and Aβ40/Aβ42 ratios were determined in brain microvascular extracts by ELISA. A threefold higher Aβ40/Aβ42 ratio was observed in brain microvessel extracts compared to whole homogenates from the same parietal cortex samples. Data are represented as mean ± SEM. Sample size is indicated in the graph bars. Statistical analysis: unpaired Student's *t* test. $^{**}p < 0.01$. **b–d** Immunolabeling of Aβ40 and Aβ42 following formic acid pretreatment revealed that both peptides accumulated on larger vessels at stage 4 parenchymal CAA in parietal cortex, while no immunoreactivity was observed at stage 0 parenchymal CAA. Markedly, for both stages, no signal was found in smaller capillary-like vessels. Magnification used: 20 ×. Scale bar: 20 μm

Concentrations of both Aβ40 and Aβ42 in microvessel extracts are higher in individuals with a neuropathological diagnosis of AD, and in apoE4 carriers

Before comparing groups of individuals for amyloid-related parameters investigated, it was important to determine whether major differences existed for the total amount of microvascular proteins extracted from human brain samples. Indeed, previous authors performing experiments on brain sections stained for markers of basal membrane have reported a decrease in total microvessel density in AD [21, 22]. Throughout this study, Western blot data of proteins of interest were normalized with cyclophilin B, as it was the loading control with the lowest variation between groups compared to other markers tested (β-actin, GAPDH and β-tubulin) (Table 1). Although a downward trend was noted, we did not observe a significant difference between individuals with AD and controls when assessing total levels of claudin-5 and CD31, two major endothelial markers, in microvessel extracts (Table 1).

Grouping participants according to the ABC neuropathological diagnosis revealed that microvascular concentrations of Aβ40 and Aβ42 were higher in individuals with AD compared to controls (Fig. 3a, b). However, no difference was observed for the microvascular ratio of Aβ40/Aβ42 (Fig. 3c). On the other hand, when dividing groups based on the clinical diagnosis (Fig. 3d–f), no significant differences in cerebrovascular Aβ were detected. Aβ40 and Aβ42 concentrations in vascular extracts were inversely correlated with visuospatial ability but not with other cognitive domains or global cognition (Fig. 3g–i; Table 3). Interestingly, we also observed that subjects carrying one apoE4 allele had higher concentrations of vascular Aβ40 and Aβ42 compared to non-carriers (Fig. 3j, k). Finally, given the high frequency of mixed vascular pathologies involving infarcts in AD [78] and their association to CAA [39] and cognitive function [6], we compared groups based on the presence of chronic cortical macro- and microinfarcts. We observed that the presence of chronic cortical infarcts was associated with higher concentrations of both Aβ40 and Aβ42, while no difference was noted for Aβ40/Aβ42 ratios (Table 4).

Concentrations of both Aβ40 and Aβ42 in microvessel extracts are elevated in individuals with higher stages of parenchymal CAA in the parietal cortex

Aβ42 levels in microvessel extracts were greater in subjects given a parenchymal CAA stage of 3 or 4 in parietal cortex compared to those without parenchymal CAA (stage 0), while a trend towards greater Aβ40 concentrations in individuals with advanced parenchymal CAA was noted (Fig. 4a, b). No difference was found between groups for the Aβ40/Aβ42 ratios (Fig. 4c). We extended our analysis by grouping participants based on the ABC neuropathological diagnosis and by subdividing them based on whether or not they were rated as having parenchymal CAA in the parietal cortex, regardless of severity. We noted that AD was associated with a rise in vascular Aβ40 and Aβ42, while parenchymal CAA was associated with higher vascular Aβ42 concentrations (Fig. 4e). Nonetheless, the highest levels for both Aβ40 and Aβ42 were found in participants with AD and parenchymal CAA, for which Aβ40 concentrations were sixfold greater than participants with AD and no parenchymal CAA (Fig. 4d, e). In addition, despite a lack of statistical significance, we found an upward trend for the cerebrovascular ratio of Aβ40/Aβ42 in volunteers with AD and parenchymal CAA (Fig. 4f). Similar observations were made following analyses in detergent-insoluble vascular fractions, where AD was also associated with greater concentrations of Aβ40 and Aβ42 (Suppl. Figure 1a, b).

The Aβ efflux transporter ABCB1 is reduced in participants with a clinical diagnosis of AD and is correlated to cognitive function and Aβ content in brain microvessels

The accumulation of Aβ in the brain parenchyma has been hypothesized to be caused by defects in its clearance through the BBB, implicating transporters and receptors expressed in brain microvascular endothelial cells [108, 111]. We thus quantified, in microvessel-enriched extracts, Aβ transporters and receptors reported to be involved in efflux or influx of Aβ across the BBB. When groups were distinguished based on the clinical diagnosis, we observed lower ABCB1 levels in persons with AD compared to NCI and MCI (Fig. 5c). In addition, ABCB1 levels were positively correlated to global cognition, episodic memory, semantic memory, perceptual speed and visuospatial ability (Fig. 5d, e; Table 3). On the other hand, vascular levels of LRP1 and RAGE, respectively, involved in the efflux or influx of Aβ across the BBB, remained similar among clinical diagnostic groups (Fig. 5j, o). Nevertheless, we noted that LRP1 levels were positively associated with global cognition, semantic memory, perceptual speed and visuospatial ability (Table 3). Levels of ABCB1, LRP1 and RAGE were similar between individuals with a neuropathological diagnosis of AD compared to controls (Fig. 5b, i, n). As indicated in Table 4, RAGE levels were significantly increased in participants with AD and chronic cortical infarcts compared to persons with AD without infarcts, whereas no difference was noted for ABCB1 and LRP1. However, no difference was observed when groups were compared based on the apoE4 carriage or parenchymal CAA stage in the parietal cortex, for all transporters and receptors investigated (not shown). A negative association was found between ABCB1 and Aβ40 in microvessel extracts (Fig. 5f). No significant correlation was found for RAGE or LRP1 (Fig. 5k, p). Moreover, we did not observe any significant correlation between Aβ transporters and receptors and Aβ42 levels in microvessel extracts (Fig. 5g, l, q).

The Aβ-degrading enzyme neprilysin is reduced in microvessel extracts from AD individuals and is correlated to cognition and Aβ40 concentrations

Enzymatic degradation is also thought to be a major clearance pathway for Aβ in the brain, also active in the vasculature [23, 36]. We noted a significant decrease in levels of neprilysin in microvessel-enriched extracts from participants clinically diagnosed with AD (Fig. 6b), but not after grouping according to autopsy-confirmed diagnoses (Fig. 6a). Moreover, vascular neprilysin levels were positively associated with global cognition, semantic memory and perceptual speed (Fig. 6c, d; Table 3). No difference was observed when participants were differentiated based on their apoE4 carriage or parenchymal CAA stage in the parietal cortex (not shown). As indicated in Table 4, neprilysin levels in brain microvessels were not altered in participants rated as having chronic cortical infarcts. A trend towards a negative correlation between neprilysin and Aβ40 in microvessel extracts was found (Fig. 6e), while no correlation was noted with Aβ42 (Fig. 6f).

The amyloid protein precursor cleaving enzyme β-secretase is elevated in microvessel extracts from participants with AD and apoE4 carriers and is correlated to cognition and Aβ concentrations

Although neurons display the strongest expression of amyloid protein precursor (APP) and produce the bulk of cerebral Aβ, APP expression and processing have been detected in brain microvascular cells in humans and rodents [30, 52, 72, 105]. We thus evaluated APP and β-secretase (BACE1) levels by WB as a potential mechanism underlying variations in vascular Aβ. We observed higher BACE1 levels in participants with a neuropathological or a clinical diagnosis

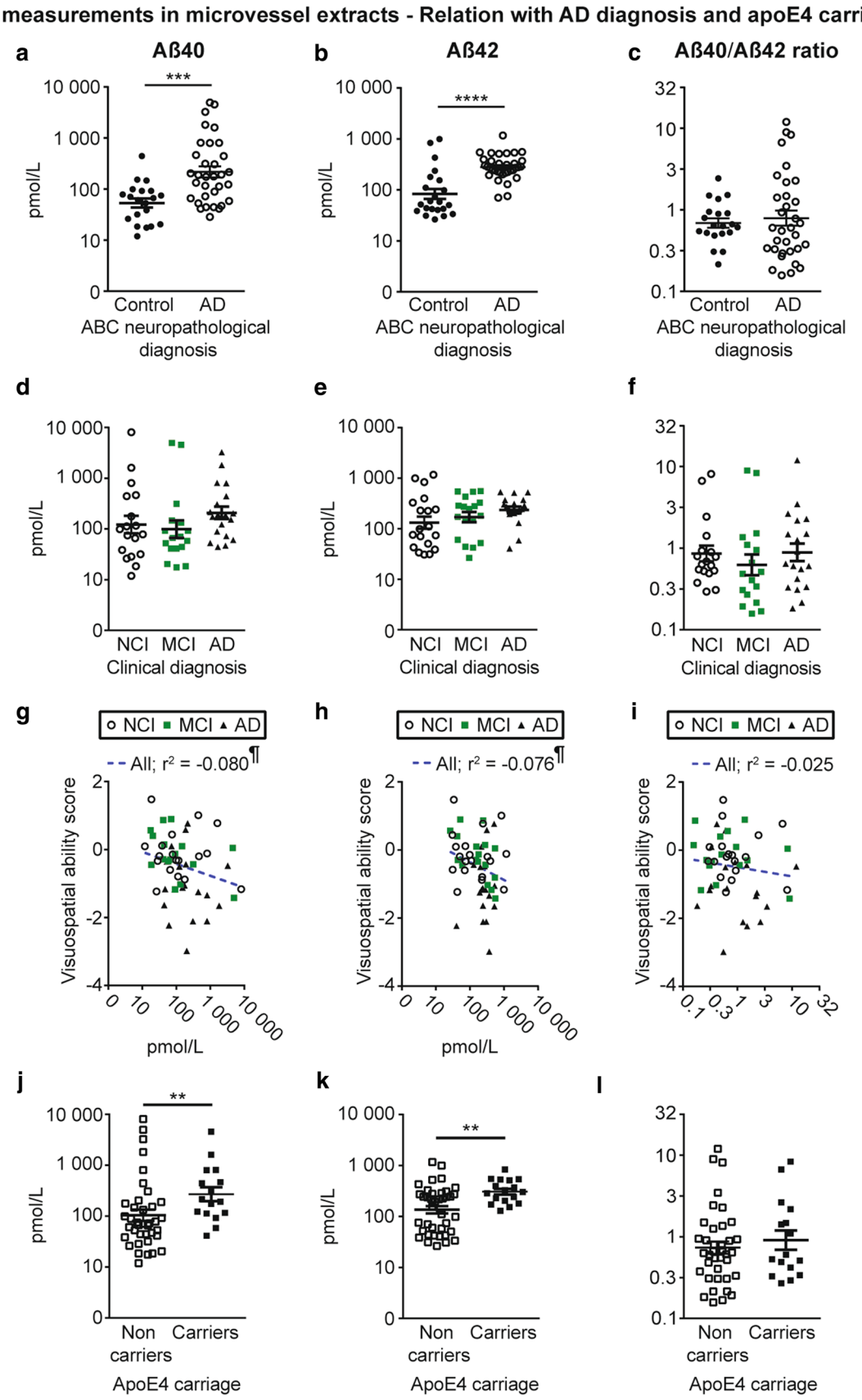
Aß measurements in microvessel extracts - Relation with AD diagnosis and apoE4 carriage
a
Aß40
b
Aß42
c
Aß40/Aß42 ratio
***
****
pmol/L
10 000
1 000
100
10
0
32
10
3
1
0.3
0.1
Control
AD
ABC neuropathological diagnosis
d
e
f
NCI
MCI
AD
Clinical diagnosis
g
h
i
NCI MCI AD
All; r² = -0.080¶
All; r² = -0.076¶
All; r² = -0.025
Visuospatial ability score
2
0
-2
-4
0
10
100
1 000
10 000
0.1
0.3
1
3
10
32
pmol/L
j
k
l
**
Non carriers
Carriers
ApoE4 carriage

◂**Fig. 3** Aβ40 and Aβ42 concentrations in brain microvessels are increased in persons with AD and in apoE4 carriers. Concentrations of Aβ40, Aβ42 and Aβ40/Aβ42 ratios were determined in brain microvascular extracts by ELISA. **a**–**c** Participants were divided according to their neuropathological diagnosis based on the ABC criteria; **d**–**f** their clinical diagnosis and **j**–**l** their apoE4 allele carriage. Higher concentrations of Aβ were observed in individuals with a neuropathological diagnosis of AD (**a**, **b**) and in apoE4 carriers (**j**, **k**). For all groups, no significant variation was found for the Aβ40/Aβ42 ratios (**c**, **f**, **l**). Data were log transformed for statistical analysis and are represented as scatter plots with a logarithmic scale. Horizontal bars indicate mean ± SEM. Statistical analysis: Mann–Whitney test. $^{**}p < 0.01$, $^{***}p < 0.001$, $^{****}p < 0.0001$. Correlative analyses revealed that Aβ40 and Aβ42 levels in microvessel extracts were both negatively associated with visuospatial ability scores (**g**, **h**). Statistical analysis: Coefficient of determination (r^2). $^{¶}p < 0.05$. *AD* Alzheimer's disease, *MCI* mild cognitive impairment, *NCI* healthy controls with no cognitive impairment

of AD (Fig. 8a, b) and in apoE4 carriers (Fig. 8c), while similar non-significant trends were found for APP in the same groups (Fig. 7a–c). In addition, we noted trends for increased APP and BACE1 levels in individuals with AD and chronic cortical infarcts (Table 4). However, no difference was observed when individuals were grouped based on their parenchymal CAA stage in the parietal cortex (not shown). BACE1 levels in microvessel extracts were negatively associated with global cognition and specific cognitive domains, namely episodic memory and perceptual speed (Fig. 8d, e and Table 3), while APP levels were negatively correlated with working memory, with trends for global cognition ($r^2 = -0.063$; $p = 0.0665$) and visuospatial ability ($r^2 = -0.065$; $p = 0.07$) (Table 3). Both APP and BACE1 were positively correlated to vascular Aβ40 concentrations (Figs. 7d, 8f). APP levels were also associated with vascular Aβ42 (Fig. 7e), while only a trend was found for BACE1 (Fig. 8g). Finally, we observed strong inverse relationships between vascular BACE1 and ABCB1 ($r^2 = -0.549$; $p < 0.0001$) and neprilysin ($r^2 = -0.330$; $p < 0.0001$) in this cohort.

Discussion

The present work aimed to investigate vascular Aβ pathology in CAA and AD using brain extracts enriched in microvascular cells. To do so, we adapted a previously published protocol to generate microvessel-enriched extracts from frozen human parietal cortex samples from participants in the Religious Orders Study. The focus was on Aβ peptides and markers involved in their clearance and production. Overall, our data are consistent with the following conclusions: (1) it is possible to effectively concentrate human brain microvessels from frozen samples; (2) a higher Aβ40/42 ratio is found in microvessels compared to the whole brain, (3) when compared to controls, the cerebrovasculature of persons with AD shows similar levels of endothelial markers but higher concentrations in Aβ peptides, associated with changes consistent with a deficit in clearance (ABCB1 and neprilysin) and an increased production (BACE1) of Aβ by brain microvascular cells; 4) cognitive decline is associated with higher levels of BACE1 and lower concentrations of both ABCB1 and neprilysin in the brain vasculature. Such series of observations highlight that brain microvascular cells play an active role in the vascular Aβ pathology that underlies CAA and AD, and their consequent cognitive symptoms.

Advantages of the approach taken

The efficacy of the microvessel enrichment approach used in this study, starting from frozen human brain samples, was confirmed by a higher proportion of endothelial and mural markers, combined with lower levels of neuronal markers, as well as higher Aβ40/Aβ42 ratios, as previously reported in the cerebral vasculature [4, 38]. Generating homogenates enriched in brain vasculature offers the possibility of using biochemical techniques more suitable for quantification in solution, such as ELISAs, Western immunoblotting and enzymatic assays. ELISA is now considered a standard and sensitive technique to specifically assess Aβ40 and Aβ42 concentrations in the CSF and other fluids [33, 57, 73], and determine Aβ40/Aβ42 ratios. Western analysis confirms protein sizes, therefore reducing bias from non-specific signals from primary and secondary antibodies. In addition, microvessel-enriched extracts facilitate the investigation of proteins located in the cerebrovasculature, including those expressed at low levels by brain microvascular cells, such as endothelial cells, while avoiding signal dilution among other cell types. Finally, compared to fresh tissue, which have to be processed when collected at autopsy, frozen brain samples can be stored and are suitable for quantitative comparisons of a large number of samples.

Vascular amyloid pathology: its relation with clinical and neuropathological AD

In the present study, we did not observe a significant reduction in the total amount of microvessels or capillaries as indexed by Western blot measurements of cyclophilin B, claudin-5 or CD31 in microvessel extracts in subjects with a neuropathological diagnosis of AD (Table 1), suggesting no massive change in the total microvascular compartment. This is consistent with a previous report showing similar CD31 staining in AD versus controls [59]. Claudin-5 and CD31 are both involved in intercellular junctions and expressed mostly in brain microvascular endothelial cells [27, 93]. It is important however to consider that each microvessel marker may give different information. For example, in postmortem AD brains, levels of von Willebrand factor (vWF), a

Table 3 Linear regressions between amyloid-related markers in brain microvessels and antemortem cognitive evaluation

	Global cognitive score	Episodic memory	Semantic memory	Perceptual speed	Visuospatial ability	Working memory
β–amyloid peptide	r^2	r^2	r^2	r^2	r^2	r^2
Aβ40, pmol/L	– 0.022	– 0.006	– 0.011	– 0.028	– 0.080	– 0.004
Aβ42, pmol/L	– 0.043	– 0.038	– 0.023	– 0.016	– 0.076	– 0.019
Aβ40/Aβ42	– 0.001	0.003	< – 0.001	– 0.020	– 0.025	< 0.001
β–amyloid peptide transporters	r^2	r^2	r^2	r^2	r^2	r^2
ABCB1 (normalized ROD)	0.154	0.101	0.147	0.149	0.090	0.057
LRP1 (normalized ROD)	0.103	0.068	0.105	0.118	0.099	0.029
RAGE (normalized ROD)	– 0.023	– 0.010	– 0.023	–0.009	‘– 0.069	– 0.013
Aβ–degrading enzymes	r^2	r^2	r^2	r^2	r^2	r^2
Neprilysin (normalized ROD)	0.090	0.030	0.105	0.166	0.050	0.051
APP processing	r^2	r^2	r^2	r^2	r^2	r^2
APP (normalized ROD)	– 0.063	– 0.052	– 0.055	– 0.043	– 0.065	– 0.076
BACE1 (normalized ROD)	– 0.108	– 0.090	– 0.073	– 0.136	– 0.015	– 0.028

ABCB1 *P*-glycoprotein, *APP* amyloid protein precursor, *BACE1* β-secretase, *LRP1* low-density lipoprotein receptor-related protein 1, *RAGE* receptor for advanced glycation end products, *ROD* relative optical density

Correlations were adjusted for the following covariates: educational level, gender, age at death and *APOE* genotype. Linear regressions were performed to generate coefficients of determination (r^2). Blue and orange highlighted cells, respectively, indicate significant positive and negative correlations with a $p < 0.05$ (light colors) and $p < 0.01$ (dark colors)

Table 4 Impact of chronic cortical infarcts on vascular amyloid

	Controls		AD		Two-way ANOVA (p values for infarcts effect)
	No infarcts	With infarcts	No infarcts	With infarcts	
	$N = 16$	$N = 6$	$N = 26$	$N = 8$	
β-Amyloid peptide					
Aβ40, pmol/L	45.6. ± 9.30	181.6 ± 184.2$^{\#}$	191.0 ± 57.9	347.5 ± 174.0$^{\#}$	0.0316
Aβ42, pmol/L	65.6 ± 12.6	158.5 ± 108.0$^{\#\&}$	264.2 ± 30.7	336.5 ± 55.6$^{\#}$	0.0221
Aβ40/Aβ42	0.66 ± 0.11	1.15 ± 0.50	0.72 ± 0.19	1.10 ± 0.48	0.1689
β-Amyloid peptide transporters					
ABCB1 (normalized ROD)	2.63 ± 0.33	2.42 ± 0.63	1.99 ± 0.20	1.72 ± 0.45	0.5308
LRP1 (normalized ROD)	3.07 ± 0.13	2.78 ± 0.16	2.87 ± 0.12	3.12 ± 0.20	0.9228
RAGE (normalized ROD)	0.89 ± 0.14	0.72 ± 0.23	0.71 ± 0.09	1.35 ± 0.24$^{\&\&}$	0.1624
Aβ-Degrading enzymes					
Neprilysin (normalized ROD)	0.41 ± 0.04	0.41 ± 0.11	0.36 ± 0.04	0.31 ± 0.04	0.1324
APP processing					
APP (normalized ROD)	0.70 ± 0.13	0.77 ± 0.26	1.11 ± 0.20	1.75 ± 0.40	0.2010
BACE1 (normalized ROD)	1.16 ± 0.20	1.45 ± 0.47	1.68 ± 0.18	2.45 ± 0.56	0.1068

ABCB1 *P*-glycoprotein, *APP* amyloid protein precursor, *BACE1* β-secretase, *LRP1* low-density lipoprotein receptor-related protein 1, *RAGE* receptor for advanced glycation end products, *ROD* relative optical density

Measurements of vascular Aβ40 and Aβ42 were performed by ELISA. Data were log transformed for statistical analysis and are represented as mean ± SEM. All other measurements were performed by Western immunoblotting. Data were normalized with cyclophilin B and are represented as mean ± SEM. The sample size for each group is indicated at the top of each column. Statistical analysis: two-way analysis of variance followed by a Bonferroni's post hoc test, $^{\#}p < 0.05$ for infarcts effect, $^{\&}p < 0.05$ and $^{\&\&}p < 0.01$ compared to individuals without infarcts within each neuropathological diagnosis group

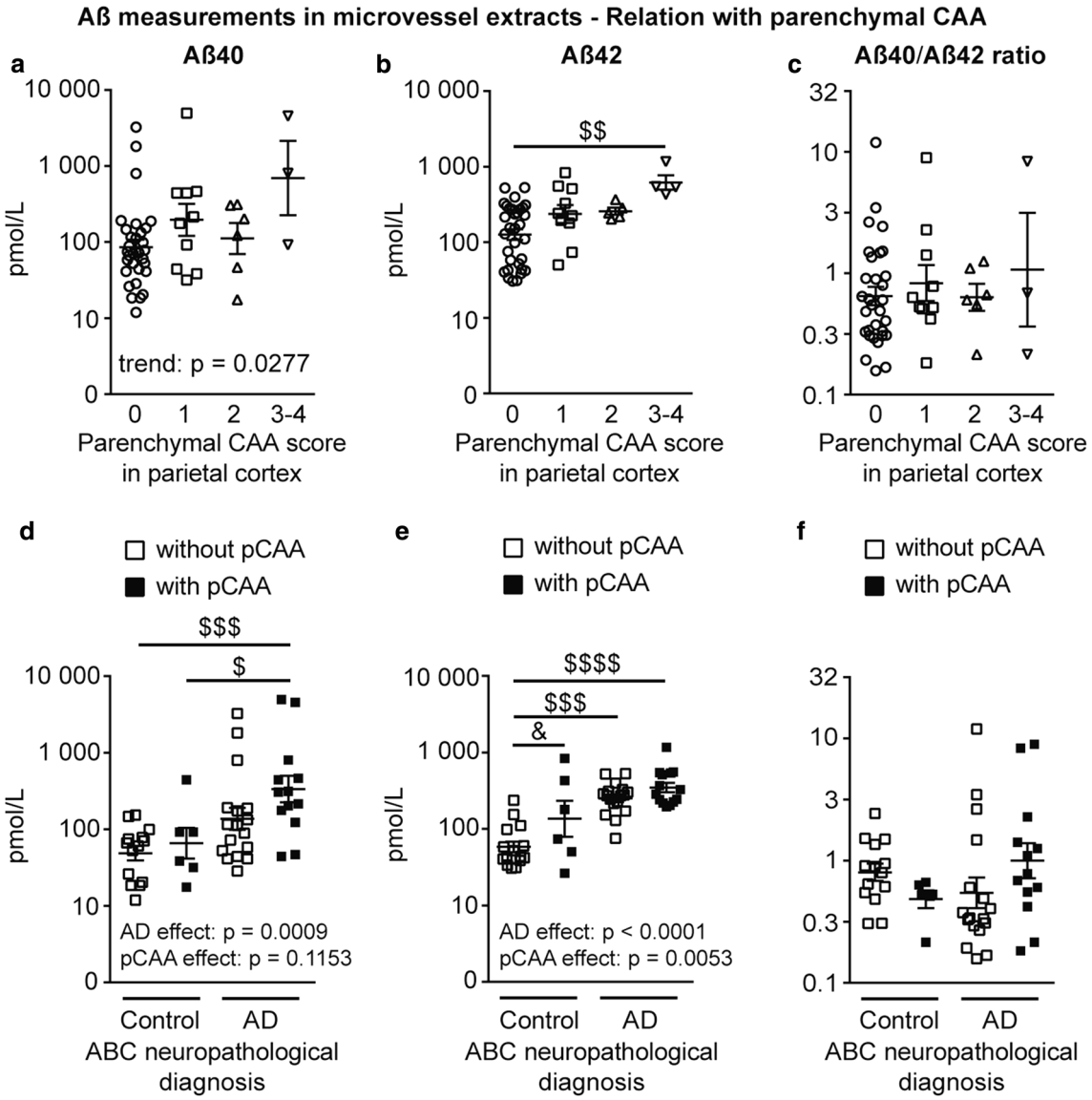

Fig. 4 Aβ40 and Aβ42 concentrations in brain microvessels are increased in participants with higher stages of parenchymal CAA in the parietal cortex. Concentrations of Aβ40, Aβ42 and Aβ40/Aβ42 ratios were determined in brain microvascular extracts by ELISA. **a**–**c** Participants were divided according to their parenchymal CAA staging in the parietal cortex as following: 0, no deposition; 1, scattered segmental but not circumferential deposition; 2, circumferential deposition up to ten vessels; 3, circumferential deposition up to 75% of the region; 4, circumferential deposition over 75% of the total region. Stages 3 and 4 were pooled together for statistical analysis. Aβ42 concentrations were elevated in individuals with stage 3 and 4 parenchymal CAA (**b**), while only an upward trend was noted for Aβ40 concentrations in the same group (**a**). Statistical analysis: Kruskal–Wallis non-parametric one-way analysis of variance followed by a Dunn's post hoc test. $^{\$\$}p < 0.01$. **d**–**f** Individuals were grouped based on their ABC neuropathological diagnosis and subdivided based on the presence or not of parenchymal CAA, regardless of the severity. Neuropathological diagnosis of AD was associated with higher Aβ40 and Aβ42 vascular concentrations (**d**, **e**), while parenchymal CAA was associated with increased levels of Aβ42 only (**e**). Highest concentrations of Aβ40 were found in participants with AD and parenchymal CAA. Statistical analysis: Kruskal–Wallis non-parametric one-way analysis of variance followed by a Dunn's post hoc test. $^{\$}p < 0.05$, $^{\$\$\$}p < 0.001$, $^{\$\$\$\$}p < 0.0001$ and two-way analysis of variance followed by a Bonferroni's post hoc test. $^{\&}p < 0.05$. Data were log transformed for statistical analysis and are represented as scatter plots with a logarithmic scale. Horizontal bars indicate mean ± SEM. *pCAA* parenchymal CAA

glycoprotein stored in endothelial cells, were reported to be unchanged or present in lower amounts, while type IV collagen content was shown to be increased, consistent with a thickening of the basal lamina [35, 40, 51, 59]. Comparisons between groups were made based on ABC assessment to determine a dichotomic neuropathological diagnosis (i.e., AD versus control). However, as exemplified by the overlap between groups for Braak and CERAD scores (Table 1), it

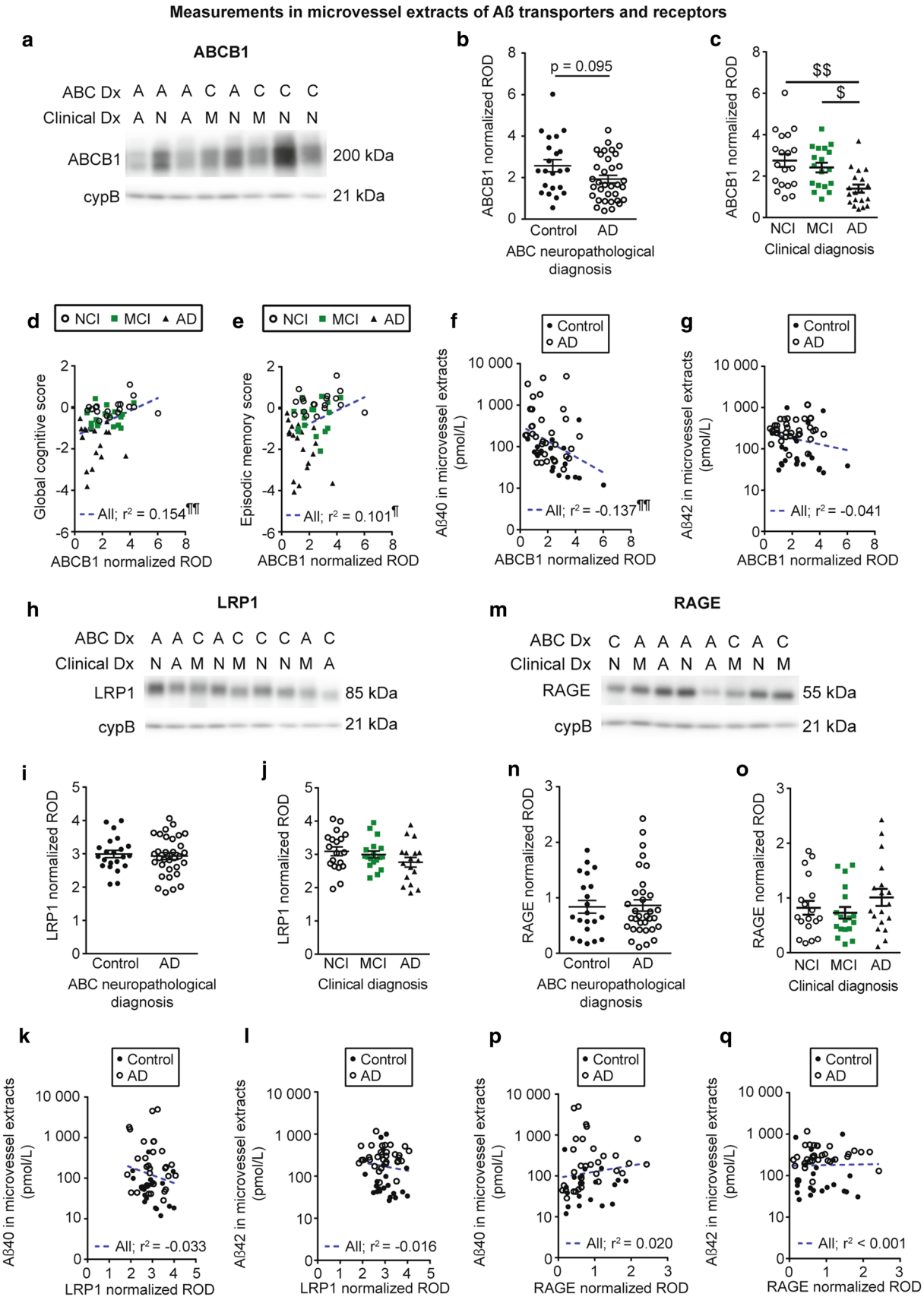
Measurements in microvessel extracts of Aß transporters and receptors
a
ABCB1
ABC Dx A A A C A C C C
Clinical Dx A N A M N M N N
ABCB1
200 kDa
cypB
21 kDa
b
p = 0.095
ABCB1 normalized ROD
Control AD
ABC neuropathological diagnosis
c
$$
$
ABCB1 normalized ROD
NCI MCI AD
Clinical diagnosis
d
NCI MCI AD
Global cognitive score
All; r² = 0.154¶¶
ABCB1 normalized ROD
e
NCI MCI AD
Episodic memory score
All; r² = 0.101¶
ABCB1 normalized ROD
f
Control AD
Aß40 in microvessel extracts (pmol/L)
All; r² = -0.137¶¶
ABCB1 normalized ROD
g
Control AD
Aß42 in microvessel extracts (pmol/L)
All; r² = -0.041
ABCB1 normalized ROD
h
LRP1
ABC Dx A A C A C C C A C
Clinical Dx N A M N M N N M A
LRP1
85 kDa
cypB
21 kDa
m
RAGE
ABC Dx C A A A A C A C
Clinical Dx N M A N A M N M
RAGE
55 kDa
cypB
21 kDa
i
LRP1 normalized ROD
Control AD
ABC neuropathological diagnosis
j
LRP1 normalized ROD
NCI MCI AD
Clinical diagnosis
n
RAGE normalized ROD
Control AD
ABC neuropathological diagnosis
o
RAGE normalized ROD
NCI MCI AD
Clinical diagnosis
k
Control AD
Aß40 in microvessel extracts (pmol/L)
All; r² = -0.033
LRP1 normalized ROD
l
Control AD
Aß42 in microvessel extracts (pmol/L)
All; r² = -0.016
LRP1 normalized ROD
p
Control AD
Aß40 in microvessel extracts (pmol/L)
All; r² = 0.020
RAGE normalized ROD
q
Control AD
Aß42 in microvessel extracts (pmol/L)
All; r² < 0.001
RAGE normalized ROD

◂**Fig. 5** Aβ efflux transporter ABCB1 is reduced in vascular fractions from individuals with AD. ABCB1 (*P*-glycoprotein), LRP1 and RAGE levels in microvessel extracts were determined by Western blot. Data were normalized with cyclophilin B. Representative immunoblotting examples for ABCB1, LRP1 and RAGE (**a**, **h**, **m**). All samples, loaded in a random order, were run on the same immunoblot experiment for quantification. Consecutive bands are shown. No difference was found when participants were divided according to their AD neuropathological diagnosis (**b**, **i**, **n**). When individuals were grouped based on their clinical diagnosis, a significant reduction was noted for ABCB1 in AD, while no difference was observed for LRP1 and RAGE (**c**, **j**, **o**). Statistical analysis: Kruskal–Wallis one-way analysis of variance followed by a Dunn's post hoc test. $^{\$}p < 0.05$, $^{\$\$}p < 0.01$. ABCB1 levels in microvessel extracts were positively associated to global cognition and episodic memory (**d**, **e**). In microvessel extracts, among transporters investigated only ABCB1 levels were inversely correlated to Aβ40 content (**f**). No significant correlation was observed between Aβ42 concentrations in microvessel extracts and any of the transporter investigated (**g**, **l**, **q**). Statistical analysis: Coefficient of determination (r^2). $^{¶}p < 0.05$, $^{¶¶}p < 0.01$. *A/AD* Alzheimer's disease, *ABC Dx* ABC neuropathological diagnosis, *C* control, *Clinical Dx* clinical diagnosis, *cypB* cyclophilin B, *M/MCI* mild cognitive impairment, *N/NCI* healthy controls with no cognitive impairment, *ROD* relative optical density

is important to keep in mind that results of the present study could be interpreted slightly differently depending on the method used for the neuropathological diagnosis.

Despite similar levels of endothelial markers, individuals with a neuropathological diagnosis of AD had higher microvascular levels of both Aβ40 and Aβ42 compared to controls. This corroborates a previous report using Western immunoblotting for total Aβ [52]. Aβ40 and Aβ42 levels were higher in apoE4 carriers, as expected because of their greater proportion within the AD population. However, apoE4 may also have a direct effect on Aβ accumulation in the cerebral vasculature. Indeed, the clearance of apoE4-Aβ complexes through both the BBB and perivascular drainage has been shown to be reduced compared to complexes formed with other apoE isoforms [29, 43]. Such accumulation of Aβ was negatively correlated to visuospatial ability, but not to other cognitive domains, which is consistent with the involvement of the parietal cortex in this particular cognitive task [88].

The transit of Aβ across the BBB is thought to be mediated by several transporters and receptors expressed by brain microvascular endothelial cells, including ABCB1 (efflux), LRP1 (efflux) and RAGE (influx) [34, 112]. The lower concentrations of ABCB1 in individuals clinically classified as AD is in line with an increased brain entry of [11C]-verapamil, a substrate of ABCB1, in several brain regions as visualized by PET scan [91]. A stronger inverse association between vascular levels of ABCB1 with Aβ40 than with Aβ42, in agreement with a previous IHC report [96], supports the proposed key role of ABCB1 in the clearance of Aβ [26, 56]. In vitro binding studies show that Aβ40 has a higher affinity and an increased ATPase-stimulating effect for ABCB1 compared to Aβ42 [58], perhaps underlying this stronger association. ABCB1 levels were also significantly correlated to all cognitive domains evaluated except working memory, suggesting a broader role for ABCB1 at the BBB than clearance of Aβ. One potential explanation is that ABCB1 has other endogenous substrates, such as lipids, including cholesterol [37, 92, 98], for which ABCB1 is thought to transport them from the inner to the outer leaflet of the plasma membrane. Moreover, Szabady et al. [81] recently showed that ABCB1 was involved in the release of endocannabinoids from intestinal epithelial cells into the lumen, where they maintain an anti-inflammatory environment for intestinal homeostasis, notably by inhibiting the transmigration of immune cells. A similar role in brain microvascular endothelial cells is plausible as they express the cellular machinery to generate and respond to endocannabinoids [61]. Therefore, ABCB1 reduction in brain microvascular endothelial cells could lead to a deleterious alteration of membrane microdomains, which have a pivotal role in signal transduction and transcytosis, and to cerebrovascular inflammation.

Given their key role in Aβ transport, studies have aimed to determine whether RAGE and LRP1 BBB levels are modified in AD, but have so far yielded conflicting results [32, 79, 103]. In line with the report from Wilhelmus et al. [103], we did not observe any difference for persons with AD, regardless of the diagnosis distinction applied. On the contrary, Shibata et al. [79] observed a reduction of LRP1 immunolabeling in capillaries of the frontal cortex in AD brains compared to controls. However, no quantification was provided in that study. In addition, Donahue et al. [32] showed that RAGE and LRP1 were, respectively, increased and reduced in hippocampal capillaries in immunostained brain sections from AD patients. These discrepancies may originate from differences in brain regions investigated, sample size, study material or methodologies, as our immunoblotting approach allowed a more quantitative assessment of the global level of proteins in vascular extracts, as mentioned above.

Neprilysin is another key contributor to Aβ clearance [36]. In the present work, we observed lower neprilysin levels in microvessel extracts from the parietal cortex of participants clinically diagnosed with AD, but not based on the ABC neuropathological assessment or apoE4 carriage. This is to some extent consistent with a previous study showing strongly reduced vascular neprilysin in the frontal cortex of participants with AD and in apoE ε4 carriers [68]. In vitro experiments revealed that neprilysin was more effective in degrading Aβ40 than Aβ42 [80], which could explain the stronger inverse correlation between vascular levels of neprilysin with Aβ40 than with Aβ42. Significant associations with global cognitive scores and specific cognitive domains, such as semantic memory and perceptual speed, suggest an

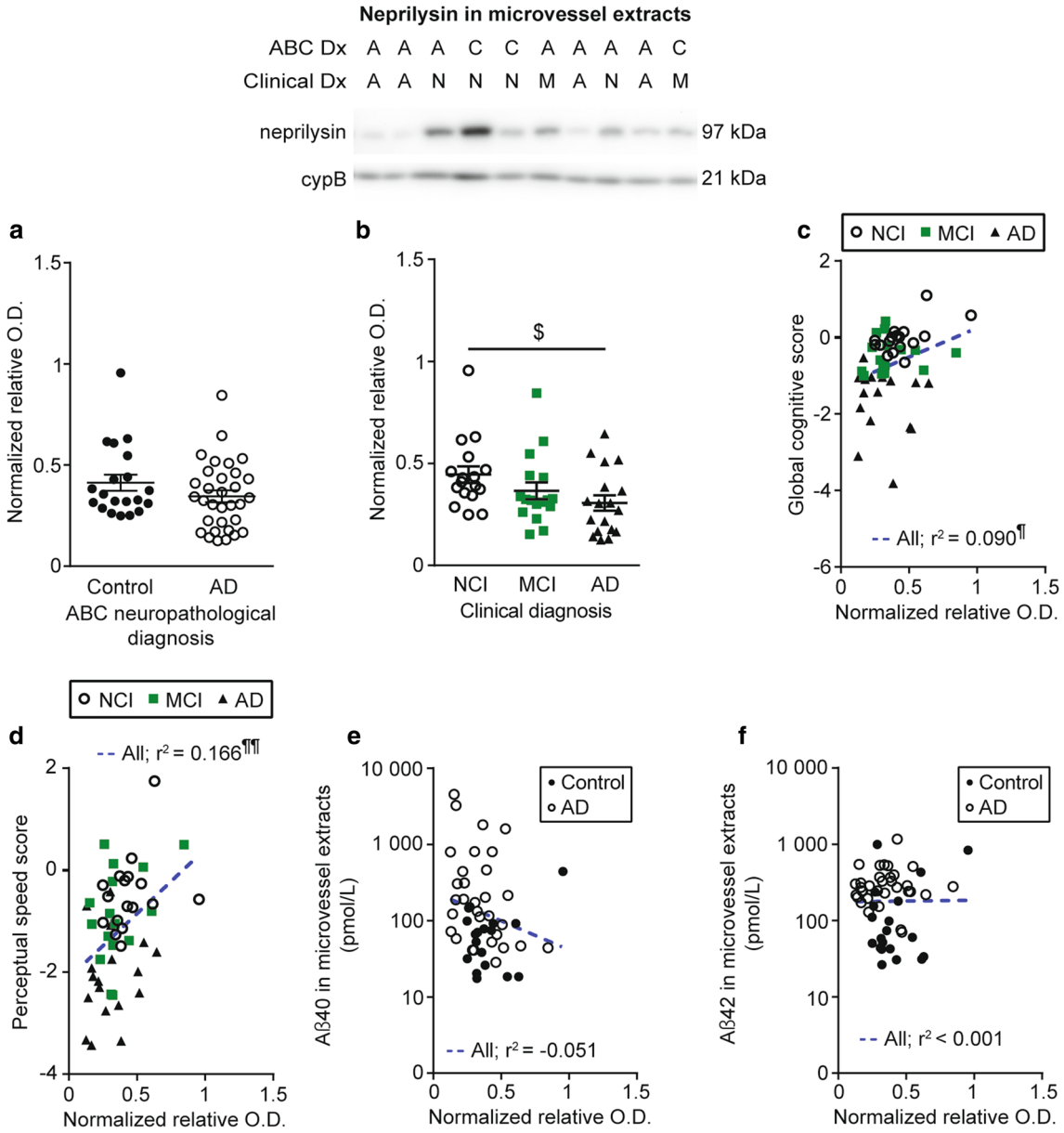

Fig. 6 Neprilysin levels are reduced in brain microvessels from individuals with AD and correlated to cognitive function and Aβ40. Neprilysin levels in microvessel extracts were determined by Western blot. Data were normalized with cyclophilin B. No difference was found when participants were divided according to their AD neuropathological assessment (**a**), while a significant decrease was observed in individuals with AD based on clinical diagnosis (**b**). All samples, loaded in a random order, were run on the same immunoblot experiment. Consecutive bands are shown. Data are represented as scatter plots. Horizontal bars indicate mean ± SEM. Statistical analysis: Kruskal–Wallis ANOVA; $^{\$}p < 0.05$. Neprilysin levels in microvessel extracts were positively associated to global cognition and perceptual speed (**c**, **d**). A trend towards a negative correlation between vascular neprilysin levels and Aβ40 (**e**) was noted, while no significant association was found with Aβ42 (**f**). Statistical analysis: Coefficient of determination (r^2). $^{¶}p < 0.05$, $^{¶¶}p < 0.01$. *A/AD* Alzheimer's disease, *ABC Dx* ABC neuropathological diagnosis, *C* control, *Clinical Dx* clinical diagnosis, *cypB* cyclophilin B, *M/MCI* mild cognitive impairment, *N/NCI* healthy controls with no cognitive impairment, *relative OD* relative optical density

extended role for cerebrovascular neprilysin in AD symptoms, other than degradation of Aβ. Indeed, neprilysin is involved in the catabolism of endothelin-1 (ET-1) [71], a potent vasoconstrictor produced by brain microvascular endothelial cells. Reduced microvascular levels of neprilysin may lead to elevated ET-1 and subsequent reduction of cerebral blood flow, often reported in AD [46, 64] and potentially contributing to cognitive decline.

A recent report shows that BACE1 is expressed in brain microvascular endothelial cells where it processes APP to

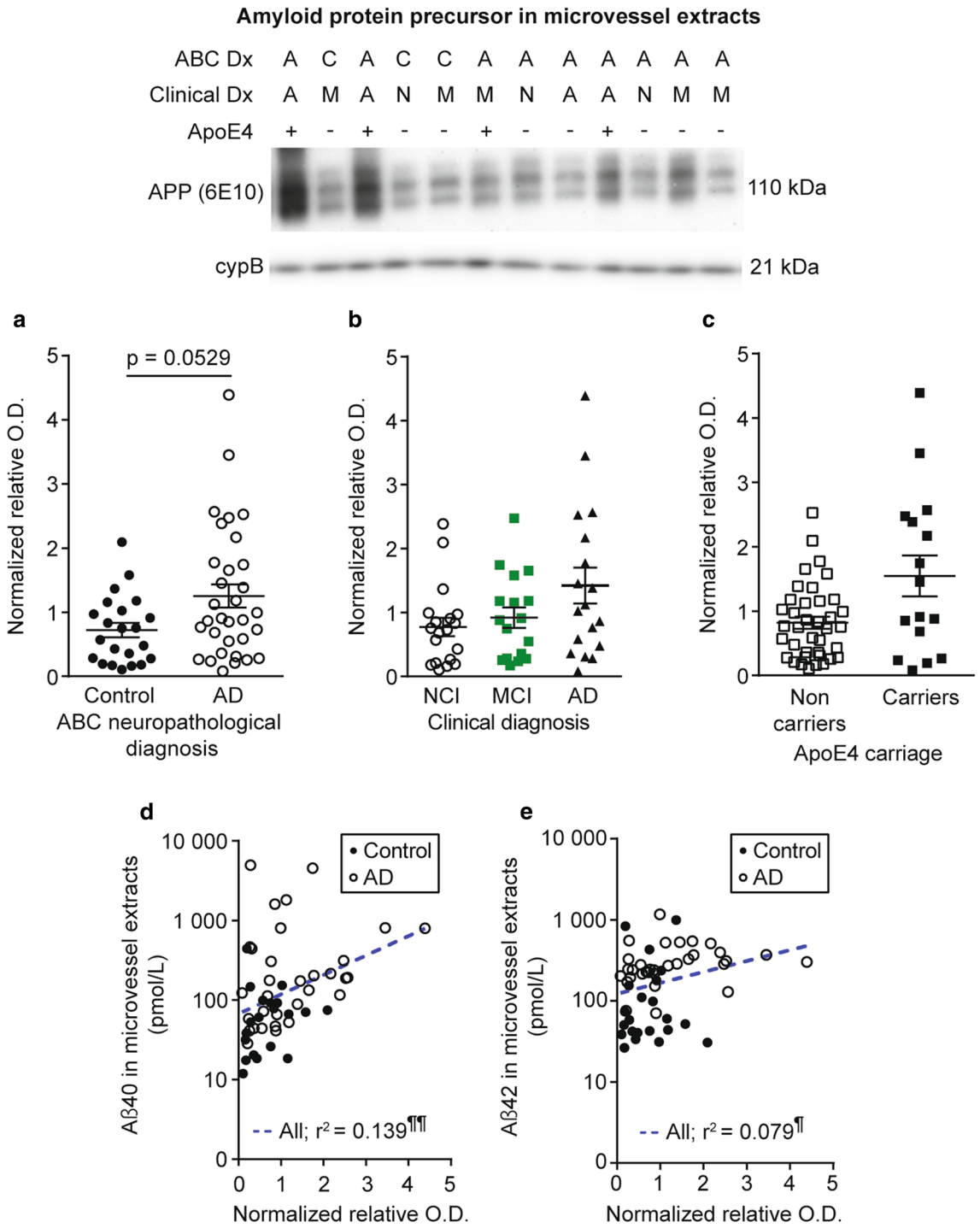

Fig. 7 Amyloid protein precursor levels are correlated to Aβ peptides concentrations in microvessel extracts. Amyloid protein precursor (APP) levels in microvessel extracts were determined by Western blot. Data were normalized with cyclophilin B. **a**–**c** Participants were divided according to **a** their AD neuropathological diagnosis; **b** their clinical diagnosis and **c** their apoE4 allele carriage. No difference was observed in any of these comparisons. All samples, loaded in a random order, were run on the same immunoblot experiment. Consecutive bands were taken for the representative photo example. Data are represented as scatter plots. Horizontal bars indicate mean ± SEM. Statistical analysis: Mann–Whitney test and Kruskal–Wallis ANOVA; $p > 0.05$. Linear regression analyses revealed that APP levels were positively correlated to both Aβ40 (**e**) and Aβ42 (**f**) concentrations in microvessel extracts. Statistical analysis: Coefficient of determination (r^2). ¶$p < 0.05$, ¶¶$p < 0.01$. − ApoE4 non-carrier, + ApoE4 carrier, *A/AD* Alzheimer's disease, *ABC Dx* ABC neuropathological diagnosis, *APP* amyloid protein precursor, *C* control, *Clinical Dx* clinical diagnosis, *cypB* cyclophilin B, *M/MCI* mild cognitive impairment, *N/NCI* healthy controls with no cognitive impairment, *relative OD* relative optical density

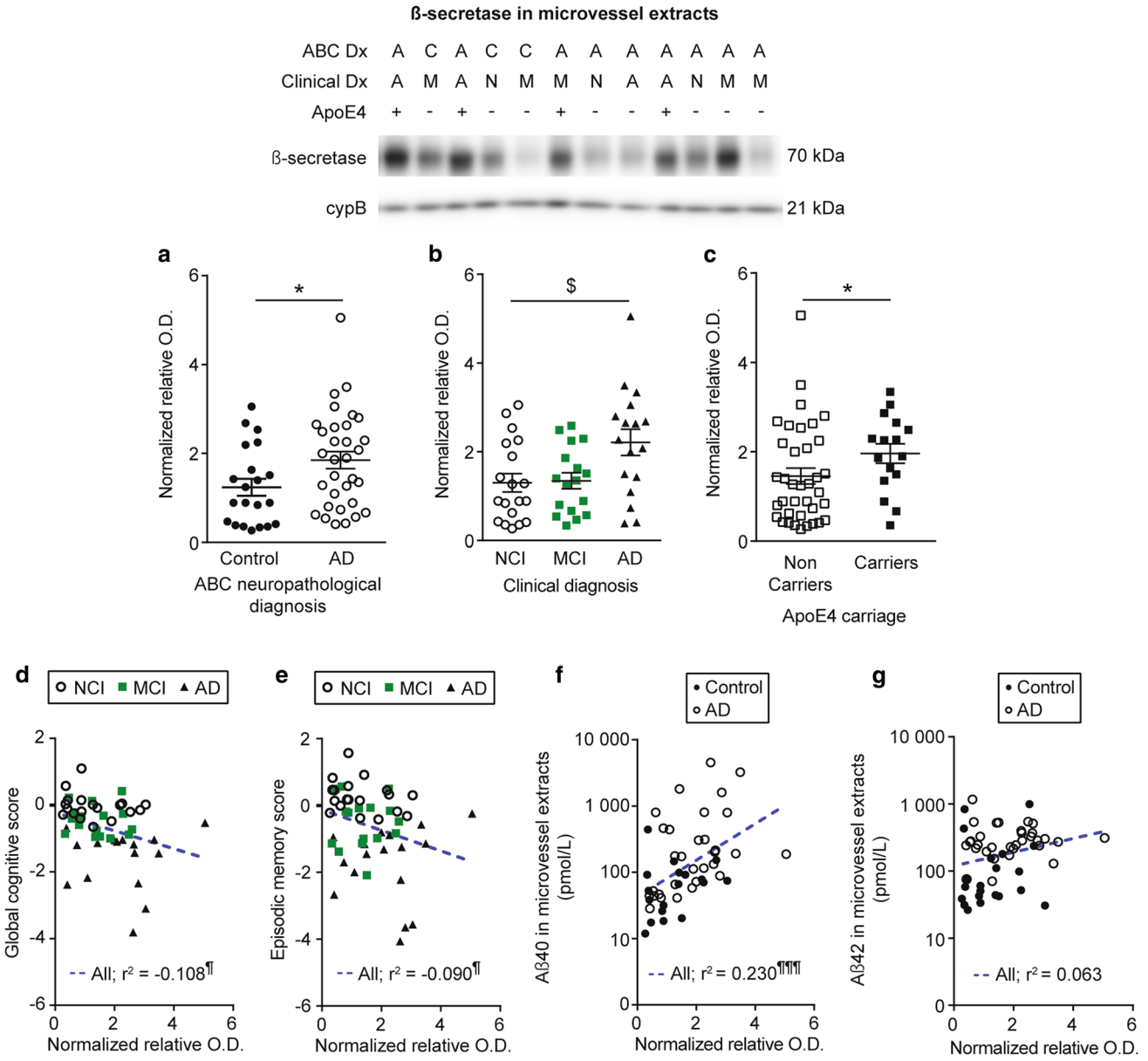

Fig. 8 β-secretase levels are increased in individuals with AD and in apoE4 carriers, and are correlated to cognition and Aβ40 peptides in microvessel extracts. β-secretase (BACE1) levels in microvessel extracts were determined by Western blot. Data were normalized with cyclophilin B. **a**–**c** Participants were divided according to **a** their AD neuropathological diagnosis; **b** their clinical diagnosis and **c** their apoE4 allele carriage. We observed an increase in BACE1 levels in individuals with a neuropathological diagnosis of AD (**a**) or a clinical diagnosis of AD (**b**). We also observed an increase for apoE4 carriers compared to non-carriers (**c**). All samples, loaded in a random order, were run on the same immunoblot experiment. Consecutive bands were taken for the representative photo example. Data are represented as scatter plots. Horizontal bars indicate mean ± SEM. Statistical analysis: Mann–Whitney test, $^{*}p < 0.05$; Kruskal–Wallis one-way analysis of variance followed by a Dunn's post hoc test, $^{\$}p < 0.05$. Linear regression analyses showed that BACE1 levels were negatively associated with global cognition (**d**) and episodic memory (**e**). In addition, BACE1 levels were positively correlated to Aβ40 concentrations in microvessel extracts (**f**). In addition, a trend towards a positive correlation was observed for Aβ42 (**g**). Statistical analysis: Coefficient of determination (r^2). $^{¶}p < 0.05$, $^{¶¶¶}p < 0.001$. − ApoE4 non-carrier, + ApoE4 carrier, *A/AD* Alzheimer's disease, *ABC Dx* ABC neuropathological diagnosis, *C* control, *Clinical Dx* clinical diagnosis, *cypB* cyclophilin B, *M/MCI* mild cognitive impairment, *N/NCI* healthy controls with no cognitive impairment, *relative OD* relative optical density

generate Aβ [30]. In accordance with this observation, we found higher levels of APP and BACE1 in brain microvessels from persons with AD, consistent with a microvascular production of Aβ. Cerebrovascular levels of BACE1 were also associated with the antemortem global cognitive scores and specific cognitive domains, notably with episodic

memory and perceptual speed, suggesting a larger implication of vascular BACE1 in BBB pathology, not limited to Aβ production. Type II interleukin-1 receptor (IL1-R2), a positive regulator of proinflammatory cytokine expression in its intracellular form [63], was shown to be upregulated in brain microvessels from AD cases compared to controls [99]. As BACE1 is involved in the shedding of IL-1R2 into its intracellular form [55], increased vascular levels of BACE1 could contribute to the spreading of neuroinflammation in the cerebral vasculature. Consistent with the observation of higher vascular levels of APP and BACE1 in apoE4 carriers, the apoE ε4 isoform was reported to induce a higher mRNA expression of APP and secretion of Aβ peptides in cultured embryonic stem cell-derived neurons [44], suggesting a similar apoE-mediated mechanism could be in place in the cerebrovasculature.

Overall, cerebrovascular markers of Aβ clearance and production investigated in this study showed stronger associations with Aβ40 than with Aβ42 concentrations. Deficient ABCB1- and neprilysin-mediated clearance and increased local production may thus act as key contributors for the increase of vascular Aβ40 resulting in higher Aβ40/Aβ42 ratios specifically in the microvessels. Such accumulation of Aβ40 could have detrimental effects on brain microvascular endothelial cells, like reduction of ABCB1 protein levels and function through ubiquitination and proteasomal-dependent degradation [41]. Recently, it has been shown that while vascular ABCB1 levels are reduced in AD, their ubiquitination status is increased [42]. Aβ40 has also been shown to induce an upregulation of proinflammatory cytokine expression [97] and epigenetic changes on DNA promoters associated to the genes of neprilysin in murine brain endothelial cells, leading to its reduced expression [25]. Finally, our results indicate that vascular levels of ABCB1, neprilysin and BACE1 were strongly correlated with Aβ40 concentrations, supporting their role in its clearance and production. Yet, Aβ40 only showed a weak correlation with visuospatial ability, while ABCB1, neprilysin and BACE1 were correlated with more cognitive domains, with stronger correlation coefficients. This suggests that the role of these markers in cognitive decline do not depend solely on their implication in the accumulation of vascular Aβ40.

Quantification of Aβ peptides in brain microvessels: interconnection between vascular pathology and AD

The present data strongly suggest that the accumulation of Aβ40 and Aβ42 in the brain microvasculature is central to the development of CAA. An apparent synergy between AD and CAA was observed as participants with a neuropathological diagnosis of AD associated with parenchymal CAA had the highest vascular concentrations of both Aβ40 and Aβ42. Such an entrapment of Aβ in the cerebrovasculature is in agreement with reports of lower Aβ40 and Aβ42 concentrations in cerebrospinal fluid of individuals with CAA [76, 94]. Despite a smaller inter-individual variability for Aβ42, the associations between Aβ40 and Aβ42 with CAA were comparable, indicating that both species remain strongly interrelated. An additive effect was observed between AD neuropathology and chronic cortical infarcts, with the highest vascular Aβ40 and Aβ42 burden measured in AD individuals with prevalent infarcts. However, only a small number of subjects with high parenchymal CAA scores or chronic cortical infarcts were included in our study, limiting the strength of our conclusions. The apoE ε4 isoform may also be a key contributor in CAA, as it was shown to alter mechanisms regulating vascular Aβ [43, 67] and to facilitate the deposition of Aβ40 [62]. In line with a role for Aβ42 in CAA, experiments in cultured microvascular cells showed that Aβ42 was associated with increased APP production and subsequent production of Aβ [28]. Thus, accumulating evidence suggest a self-stimulating loop involving Aβ, apoE4, BACE1, ABCB1 and neprilysin, which could explain the series of correlations observed here. Overall, this study pinpoints that the vascular signature of AD probably includes a complex pattern of changes (lower ABCB1 and neprilysin levels, higher BACE1 and Aβ levels) ultimately contributing to the development of CAA and cognitive symptoms.

Acknowledgements Funding was provided by the Canadian Institutes of Health Research (CIHR) to F.C (MOP 125930). The study was supported in part by P30AG10161 and R01AG15819 (D.A.B). F.C is a Fonds de recherche du Québec-Santé (FRQ-S) senior research scholar. P.B held scholarships from the Réseau québécois de recherche sur le médicament (RQRM), Fondation du CHU de Québec and a joined scholarship from the FRQ-S and the Alzheimer Society of Canada (ASC) and now holds a scholarship from the CIHR. The authors are thankful to Gregory Klein, from the Rush Alzheimer's Disease Research Center, for his assistance with data related to our cohort. The authors are indebted to the nuns, priests and brothers from the Catholic clergy participating in the Religious Orders Study. The authors are thankful to Dr. Vincent Émond for his proofreading of the manuscript.

Compliance with ethical standards

Conflict of interest The authors declare that they have no conflict of interest.

Ethical approval All procedures performed in studies involving human participants were in accordance with the ethical standards of the institutional and/or national research committee and with the 1964 Helsinki Declaration and its later amendments or comparable ethical standards.

Informed consent Informed consent was obtained from all individual participants included in the study.

References

1. Aggarwal NT, Wilson RS, Beck TL, Bienias JL, Bennett DA (2005) Mild cognitive impairment in different functional domains and incident Alzheimer's disease. J Neurol Neurosurg Psychiatry 76:1479–1484
2. Alata W, Paris-Robidas S, Emond V, Bourasset F, Calon F (2014) Brain uptake of a fluorescent vector targeting the transferrin receptor: a novel application of in situ brain perfusion. Mol Pharm 11:243–253
3. Alata W, Ye Y, St-Amour I, Vandal M, Calon F (2015) Human apolipoprotein E varepsilon4 expression impairs cerebral vascularization and blood–brain barrier function in mice. J Cereb Blood Flow Metab 35:86–94
4. Alonzo NC, Hyman BT, Rebeck GW, Greenberg SM (1998) Progression of cerebral amyloid angiopathy: accumulation of amyloid-beta40 in affected vessels. J Neuropathol Exp Neurol 57:353–359
5. Arvanitakis Z, Grodstein F, Bienias JL, Schneider JA, Wilson RS, Kelly JF et al (2008) Relation of NSAIDs to incident AD, change in cognitive function, and AD pathology. Neurology 70:2219–2225
6. Arvanitakis Z, Leurgans SE, Barnes LL, Bennett DA, Schneider JA (2011) Microinfarct pathology, dementia, and cognitive systems. Stroke 42:722–727
7. Arvanitakis Z, Leurgans SE, Wang Z, Wilson RS, Bennett DA, Schneider JA (2011) Cerebral amyloid angiopathy pathology and cognitive domains in older persons. Ann Neurol 69:320–327
8. Arvanitakis Z, Schneider JA, Wilson RS, Bienias JL, Kelly JF, Evans DA et al (2008) Statins, incident Alzheimer disease, change in cognitive function, and neuropathology. Neurology 70:1795–1802
9. Attems J, Lintner F, Jellinger KA (2004) Amyloid beta peptide 1-42 highly correlates with capillary cerebral amyloid angiopathy and Alzheimer disease pathology. Acta Neuropathol 107:283–291
10. Bell RD, Zlokovic BV (2009) Neurovascular mechanisms and blood–brain barrier disorder in Alzheimer's disease. Acta Neuropathol 118:103–113
11. Bennett DA (2006) Postmortem indices linking risk factors to cognition: results from the religious order study and the memory and aging project. Alzheimer Dis Assoc Disord 20:S63–S68
12. Bennett DA, Schneider JA, Aggarwal NT, Arvanitakis Z, Shah RC, Kelly JF et al (2006) Decision rules guiding the clinical diagnosis of Alzheimer's disease in two community-based cohort studies compared to standard practice in a clinic-based cohort study. Neuroepidemiology 27:169–176
13. Bennett DA, Schneider JA, Arvanitakis Z, Kelly JF, Aggarwal NT, Shah RC et al (2006) Neuropathology of older persons without cognitive impairment from two community-based studies. Neurology 66:1837–1844
14. Bennett DA, Schneider JA, Arvanitakis Z, Wilson RS (2012) Overview and findings from the religious orders study. Curr Alzheimer Res 9:628–645
15. Bennett DA, Schneider JA, Bienias JL, Evans DA, Wilson RS (2005) Mild cognitive impairment is related to Alzheimer disease pathology and cerebral infarctions. Neurology 64:834–841
16. Bennett DA, Wilson RS, Schneider JA, Evans DA, Beckett LA, Aggarwal NT et al (2002) Natural history of mild cognitive impairment in older persons. Neurology 59:198–205
17. Biffi A, Greenberg SM (2011) Cerebral amyloid angiopathy: a systematic review. J Clin Neurol 7:1–9
18. Boulay AC, Saubamea B, Decleves X, Cohen-Salmon M (2015) Purification of Mouse Brain Vessels. J Vis Exp e53208
19. Boyle PA, Yu L, Nag S, Leurgans S, Wilson RS, Bennett DA et al (2015) Cerebral amyloid angiopathy and cognitive outcomes in community-based older persons. Neurology 85:1930–1936
20. Braak H, Braak E (1991) Neuropathological staging of Alzheimer-related changes. Acta Neuropathol 82:239–259
21. Buee L, Hof PR, Bouras C, Delacourte A, Perl DP, Morrison JH et al (1994) Pathological alterations of the cerebral microvasculature in Alzheimer's disease and related dementing disorders. Acta Neuropathol 87:469–480
22. Buee L, Hof PR, Delacourte A (1997) Brain microvascular changes in Alzheimer's disease and other dementias. Ann N Y Acad Sci 826:7–24
23. Carpentier M, Robitaille Y, DesGroseillers L, Boileau G, Marcinkiewicz M (2002) Declining expression of neprilysin in Alzheimer disease vasculature: possible involvement in cerebral amyloid angiopathy. J Neuropathol Exp Neurol 61:849–856
24. Caselli RJ, Walker D, Sue L, Sabbagh M, Beach T (2010) Amyloid load in nondemented brains correlates with APOE e4. Neurosci Lett 473:168–171
25. Chen KL, Wang SS, Yang YY, Yuan RY, Chen RM, Hu CJ (2009) The epigenetic effects of amyloid-beta(1-40) on global DNA and neprilysin genes in murine cerebral endothelial cells. Biochem Biophys Res Commun 378:57–61
26. Cirrito JR, Deane R, Fagan AM, Spinner ML, Parsadanian M, Finn MB et al (2005) *P*-glycoprotein deficiency at the blood–brain barrier increases amyloid-beta deposition in an Alzheimer disease mouse model. J Clin Invest 115:3285–3290
27. Dai M, Lin Y, El-Amouri SS, Kohls M, Pan D (2018) Comprehensive evaluation of blood–brain barrier-forming micro-vasculatures: reference and marker genes with cellular composition. PLoS One 13:e0197379
28. Davis-Salinas J, Saporito-Irwin SM, Cotman CW, Van Nostrand WE (1995) Amyloid beta-protein induces its own production in cultured degenerating cerebrovascular smooth muscle cells. J Neurochem 65:931–934
29. Deane R, Sagare A, Hamm K, Parisi M, Lane S, Finn MB et al (2008) apoE isoform-specific disruption of amyloid beta peptide clearance from mouse brain. J Clin Invest 118:4002–4013
30. Devraj K, Poznanovic S, Spahn C, Schwall G, Harter PN, Mittelbronn M et al (2016) BACE-1 is expressed in the blood–brain barrier endothelium and is upregulated in a murine model of Alzheimer's disease. J Cereb Blood Flow Metab 36:1281–1294
31. Do TM, Alata W, Dodacki A, Traversy MT, Chacun H, Pradier L et al (2014) Altered cerebral vascular volumes and solute transport at the blood–brain barriers of two transgenic mouse models of Alzheimer's disease. Neuropharmacology 81:311–317
32. Donahue JE, Flaherty SL, Johanson CE, Duncan JA 3rd, Silverberg GD, Miller MC et al (2006) RAGE, LRP-1, and amyloid-beta protein in Alzheimer's disease. Acta Neuropathol 112:405–415
33. Engelborghs S, Maertens K, Vloeberghs E, Aerts T, Somers N, Marien P et al (2006) Neuropsychological and behavioural correlates of CSF biomarkers in dementia. Neurochem Int 48:286–295
34. Erickson MA, Banks WA (2013) Blood–brain barrier dysfunction as a cause and consequence of Alzheimer's disease. J Cereb Blood Flow Metab 33:1500–1513
35. Farkas E, Luiten PG (2001) Cerebral microvascular pathology in aging and Alzheimer's disease. Prog Neurobiol 64:575–611
36. Farris W, Schutz SG, Cirrito JR, Shankar GM, Sun X, George A et al (2007) Loss of neprilysin function promotes amyloid plaque formation and causes cerebral amyloid angiopathy. Am J Pathol 171:241–251
37. Garrigues A, Escargueil AE, Orlowski S (2002) The multidrug transporter, *P*-glycoprotein, actively mediates cholesterol redistribution in the cell membrane. Proc Natl Acad Sci USA 99:10347–10352

38. Gravina SA, Ho L, Eckman CB, Long KE, Otvos L Jr, Younkin LH et al (1995) Amyloid beta protein (A beta) in Alzheimer's disease brain. Biochemical and immunocytochemical analysis with antibodies specific for forms ending at A beta 40 or A beta 42(43). J Biol Chem 270:7013–7016
39. Haglund M, Passant U, Sjobeck M, Ghebremedhin E, Englund E (2006) Cerebral amyloid angiopathy and cortical microinfarcts as putative substrates of vascular dementia. Int J Geriatr Psychiatry 21:681–687
40. Harris R, Miners JS, Allen S, Love S (2018) VEGFR1 and VEGFR2 in Alzheimer's disease. J Alzheimers Dis 61:741–752
41. Hartz AM, Zhong Y, Wolf A, LeVine H 3rd, Miller DS, Bauer B (2016) Abeta40 reduces *P*-glycoprotein at the blood–brain barrier through the ubiquitin–proteasome pathway. J Neurosci 36:1930–1941
42. Hartz AMS, Zhong Y, Shen AN, Abner EL, Bauer B (2018) Preventing *P*-gp ubiquitination lowers Abeta brain levels in an Alzheimer's disease mouse model. Front Aging Neurosci 10:186
43. Hawkes CA, Sullivan PM, Hands S, Weller RO, Nicoll JA, Carare RO (2012) Disruption of arterial perivascular drainage of amyloid-beta from the brains of mice expressing the human APOE epsilon4 allele. PLoS One 7:e41636
44. Huang YA, Zhou B, Wernig M, Sudhof TC (2017) ApoE2, ApoE3, and ApoE4 differentially stimulate APP transcription and abeta secretion. Cell 168(427–441):e421
45. Iadecola C (2004) Neurovascular regulation in the normal brain and in Alzheimer's disease. Nat Rev Neurosci 5:347–360
46. Johnson NA, Jahng GH, Weiner MW, Miller BL, Chui HC, Jagust WJ et al (2005) Pattern of cerebral hypoperfusion in Alzheimer disease and mild cognitive impairment measured with arterial spin-labeling MR imaging: initial experience. Radiology 234:851–859
47. Julien C, Tremblay C, Bendjelloul F, Phivilay A, Coulombe MA, Emond V et al (2008) Decreased drebrin mRNA expression in Alzheimer disease: correlation with tau pathology. J Neurosci Res 86:2292–2302
48. Julien C, Tremblay C, Emond V, Lebbadi M, Salem N Jr, Bennett DA et al (2009) Sirtuin 1 reduction parallels the accumulation of tau in Alzheimer disease. J Neuropathol Exp Neurol 68:48–58
49. Kakuda N, Miyasaka T, Iwasaki N, Nirasawa T, Wada-Kakuda S, Takahashi-Fujigasaki J et al (2017) Distinct deposition of amyloid-beta species in brains with Alzheimer's disease pathology visualized with MALDI imaging mass spectrometry. Acta Neuropathol Commun 5:73
50. Kalaria RN, Harik SI (1989) Reduced glucose transporter at the blood–brain barrier and in cerebral cortex in Alzheimer disease. J Neurochem 53:1083–1088
51. Kalaria RN, Pax AB (1995) Increased collagen content of cerebral microvessels in Alzheimer's disease. Brain Res 705:349–352
52. Kalaria RN, Premkumar DR, Pax AB, Cohen DL, Lieberburg I (1996) Production and increased detection of amyloid beta protein and amyloidogenic fragments in brain microvessels, meningeal vessels and choroid plexus in Alzheimer's disease. Brain Res Mol Brain Res 35:58–68
53. Kapasi A, Schneider JA (2016) Vascular contributions to cognitive impairment, clinical Alzheimer's disease, and dementia in older persons. Biochim Biophys Acta 1862:878–886
54. Keage HA, Carare RO, Friedland RP, Ince PG, Love S, Nicoll JA et al (2009) Population studies of sporadic cerebral amyloid angiopathy and dementia: a systematic review. BMC Neurol 9:3
55. Kuhn PH, Marjaux E, Imhof A, De Strooper B, Haass C, Lichtenthaler SF (2007) Regulated intramembrane proteolysis of the interleukin-1 receptor II by alpha-, beta-, and gamma-secretase. J Biol Chem 282:11982–11995
56. Kuhnke D, Jedlitschky G, Grube M, Krohn M, Jucker M, Mosyagin I et al (2007) MDR1-*P*-Glycoprotein (ABCB1) mediates transport of Alzheimer's amyloid-beta peptides: implications for the mechanisms of Abeta clearance at the blood–brain barrier. Brain Pathol 17:347–353
57. Lachno DR, Evert BA, Vanderstichele H, Robertson M, Demattos RB, Konrad RJ et al (2013) Validation of assays for measurement of amyloid-beta peptides in cerebrospinal fluid and plasma specimens from patients with Alzheimer's disease treated with solanezumab. J Alzheimers Dis 34:897–910
58. Lam FC, Liu R, Lu P, Shapiro AB, Renoir JM, Sharom FJ, Reiner PB (2001) beta-Amyloid efflux mediated by *p*-glycoprotein. J Neurochem 76:1121–1128
59. Lepelletier FX, Mann DM, Robinson AC, Pinteaux E, Boutin H (2017) Early changes in extracellular matrix in Alzheimer's disease. Neuropathol Appl Neurobiol 43:167–182
60. Love S, Miners JS (2016) Cerebrovascular disease in ageing and Alzheimer's disease. Acta Neuropathol 131:645–658
61. Maccarrone M, Fiori A, Bari M, Granata F, Gasperi V, De Stefano ME et al (2006) Regulation by cannabinoid receptors of anandamide transport across the blood–brain barrier and through other endothelial cells. Thromb Haemost 95:117–127
62. Mann DM, Iwatsubo T, Pickering-Brown SM, Owen F, Saido TC, Perry RH (1997) Preferential deposition of amyloid beta protein (Abeta) in the form Abeta40 in Alzheimer's disease is associated with a gene dosage effect of the apolipoprotein E E4 allele. Neurosci Lett 221:81–84
63. Mar AC, Chu CH, Lee HJ, Chien CW, Cheng JJ, Yang SH et al (2015) Interleukin-1 receptor type 2 acts with c-Fos to enhance the expression of interleukin-6 and vascular endothelial growth factor A in colon cancer cells and induce angiogenesis. J Biol Chem 290:22212–22224
64. Mattsson N, Tosun D, Insel PS, Simonson A, Jack CR Jr, Beckett LA et al (2014) Association of brain amyloid-beta with cerebral perfusion and structure in Alzheimer's disease and mild cognitive impairment. Brain 137:1550–1561
65. Mawuenyega KG, Sigurdson W, Ovod V, Munsell L, Kasten T, Morris JC et al (2010) Decreased clearance of CNS beta-amyloid in Alzheimer's disease. Science 330:1774
66. Miller MC, Tavares R, Johanson CE, Hovanesian V, Donahue JE, Gonzalez L et al (2008) Hippocampal RAGE immunoreactivity in early and advanced Alzheimer's disease. Brain Res 1230:273–280
67. Miners JS, Kehoe P, Love S (2011) Neprilysin protects against cerebral amyloid angiopathy and Abeta-induced degeneration of cerebrovascular smooth muscle cells. Brain Pathol 21:594–605
68. Miners JS, Van Helmond Z, Chalmers K, Wilcock G, Love S, Kehoe PG (2006) Decreased expression and activity of neprilysin in Alzheimer disease are associated with cerebral amyloid angiopathy. J Neuropathol Exp Neurol 65:1012–1021
69. Mirra SS, Heyman A, McKeel D, Sumi SM, Crain BJ, Brownlee LM et al (1991) The Consortium to Establish a Registry for Alzheimer's Disease (CERAD). Part II. Standardization of the neuropathologic assessment of Alzheimer's disease. Neurology 41:479–486
70. Montine TJ, Phelps CH, Beach TG, Bigio EH, Cairns NJ, Dickson DW et al (2012) National Institute on Aging-Alzheimer's Association guidelines for the neuropathologic assessment of Alzheimer's disease: a practical approach. Acta Neuropathol 123:1–11
71. Nalivaeva NN, Belyaev ND, Zhuravin IA, Turner AJ (2012) The Alzheimer's amyloid-degrading peptidase, neprilysin: can we control it? Int J Alzheimers Dis 2012:383796
72. Natte R, de Boer WI, Maat-Schieman ML, Baelde HJ, Vinters HV, Roos RA et al (1999) Amyloid beta precursor protein-mRNA is expressed throughout cerebral vessel walls. Brain Res 828:179–183

73. Parnetti L, Lanari A, Silvestrelli G, Saggese E, Reboldi P (2006) Diagnosing prodromal Alzheimer's disease: role of CSF biochemical markers. Mech Ageing Dev 127:129–132
74. Pfeifer LA, White LR, Ross GW, Petrovitch H, Launer LJ (2002) Cerebral amyloid angiopathy and cognitive function: the HAAS autopsy study. Neurology 58:1629–1634
75. Piert M, Koeppe RA, Giordani B, Berent S, Kuhl DE (1996) Diminished glucose transport and phosphorylation in Alzheimer's disease determined by dynamic FDG-PET. J Nucl Med 37:201–208
76. Renard D, Castelnovo G, Wacongne A, Le Floch A, Thouvenot E, Mas J et al (2012) Interest of CSF biomarker analysis in possible cerebral amyloid angiopathy cases defined by the modified Boston criteria. J Neurol 259:2429–2433
77. Revesz T, Ghiso J, Lashley T, Plant G, Rostagno A, Frangione B et al (2003) Cerebral amyloid angiopathies: a pathologic, biochemical, and genetic view. J Neuropathol Exp Neurol 62:885–898
78. Schneider JA (2009) High blood pressure and microinfarcts: a link between vascular risk factors, dementia, and clinical Alzheimer's disease. J Am Geriatr Soc 57:2146–2147
79. Shibata M, Yamada S, Kumar SR, Calero M, Bading J, Frangione B et al (2000) Clearance of Alzheimer's amyloid-ss(1-40) peptide from brain by LDL receptor-related protein-1 at the blood–brain barrier. J Clin Invest 106:1489–1499
80. Shirotani K, Tsubuki S, Iwata N, Takaki Y, Harigaya W, Maruyama K et al (2001) Neprilysin degrades both amyloid beta peptides 1-40 and 1-42 most rapidly and efficiently among thiorphan- and phosphoramidon-sensitive endopeptidases. J Biol Chem 276:21895–21901
81. Szabady RL, Louissaint C, Lubben A, Xie B, Reeksting S, Tuohy C et al (2018) Intestinal *P*-glycoprotein exports endocannabinoids to prevent inflammation and maintain homeostasis. J Clin Invest 128:4044–4056
82. Tanskanen M, Lindsberg PJ, Tienari PJ, Polvikoski T, Sulkava R, Verkkoniemi A et al (2005) Cerebral amyloid angiopathy in a 95+ cohort: complement activation and apolipoprotein E (ApoE) genotype. Neuropathol Appl Neurobiol 31:589–599
83. Thal DR, Ghebremedhin E, Rub U, Yamaguchi H, Del Tredici K, Braak H (2002) Two types of sporadic cerebral amyloid angiopathy. J Neuropathol Exp Neurol 61:282–293
84. Thal DR, Griffin WS, de Vos RA, Ghebremedhin E (2008) Cerebral amyloid angiopathy and its relationship to Alzheimer's disease. Acta Neuropathol 115:599–609
85. Thal DR, Rub U, Orantes M, Braak H (2002) Phases of A beta-deposition in the human brain and its relevance for the development of AD. Neurology 58:1791–1800
86. Thomsen MS, Routhe LJ, Moos T (2017) The vascular basement membrane in the healthy and pathological brain. J Cereb Blood Flow Metab 271678X17722436
87. Traversy MT, Vandal M, Tremblay C, Tournissac M, Giguere-Rancourt A, Bennett AD et al (2017) Altered cerebral insulin response in transgenic mice expressing the epsilon-4 allele of the human apolipoprotein E gene. Psychoneuroendocrinology 77:203–210
88. Tremblay C, Francois A, Delay C, Freland L, Vandal M, Bennett DA et al (2017) Association of neuropathological markers in the parietal cortex with antemortem cognitive function in persons with mild cognitive impairment and Alzheimer disease. J Neuropathol Exp Neurol 76:70–88
89. Tremblay C, Pilote M, Phivilay A, Emond V, Bennett DA, Calon F (2007) Biochemical characterization of Abeta and tau pathologies in mild cognitive impairment and Alzheimer's disease. J Alzheimers Dis 12:377–390
90. Tremblay C, St-Amour I, Schneider J, Bennett DA, Calon F (2011) Accumulation of transactive response DNA binding protein 43 in mild cognitive impairment and Alzheimer disease. J Neuropathol Exp Neurol 70:788–798
91. van Assema DM, Lubberink M, Bauer M, van der Flier WM, Schuit RC, Windhorst AD et al (2012) Blood–brain barrier *P*-glycoprotein function in Alzheimer's disease. Brain 135:181–189
92. van Helvoort A, Smith AJ, Sprong H, Fritzsche I, Schinkel AH, Borst P et al (1996) MDR1 *P*-glycoprotein is a lipid translocase of broad specificity, while MDR3 *P*-glycoprotein specifically translocates phosphatidylcholine. Cell 87:507–517
93. Vanlandewijck M, He L, Mae MA, Andrae J, Ando K, Del Gaudio F et al (2018) A molecular atlas of cell types and zonation in the brain vasculature. Nature 554:475–480
94. Verbeek MM, Kremer BP, Rikkert MO, Van Domburg PH, Skehan ME, Greenberg SM (2009) Cerebrospinal fluid amyloid beta(40) is decreased in cerebral amyloid angiopathy. Ann Neurol 66:245–249
95. Vinters HV (1987) Cerebral amyloid angiopathy. A critical review. Stroke 18:311–324
96. Vogelgesang S, Cascorbi I, Schroeder E, Pahnke J, Kroemer HK, Siegmund W et al (2002) Deposition of Alzheimer's beta-amyloid is inversely correlated with *P*-glycoprotein expression in the brains of elderly non-demented humans. Pharmacogenetics 12:535–541
97. Vukic V, Callaghan D, Walker D, Lue LF, Liu QY, Couraud PO, Romero IA, Weksler B, Stanimirovic DB, Zhang W (2009) Expression of inflammatory genes induced by beta-amyloid peptides in human brain endothelial cells and in Alzheimer's brain is mediated by the JNK–AP1 signaling pathway. Neurobiol Dis 34:95–106
98. Wang E, Casciano CN, Clement RP, Johnson WW (2000) Cholesterol interaction with the daunorubicin binding site of *P*-glycoprotein. Biochem Biophys Res Commun 276:909–916
99. Wang S, Qaisar U, Yin X, Grammas P (2012) Gene expression profiling in Alzheimer's disease brain microvessels. J Alzheimers Dis 31:193–205
100. Wang S, Wang R, Chen L, Bennett DA, Dickson DW, Wang DS (2010) Expression and functional profiling of neprilysin, insulin-degrading enzyme, and endothelin-converting enzyme in prospectively studied elderly and Alzheimer's brain. J Neurochem 115:47–57
101. Weller RO, Preston SD, Subash M, Carare RO (2009) Cerebral amyloid angiopathy in the aetiology and immunotherapy of Alzheimer disease. Alzheimers Res Ther 1:6
102. Wijesuriya HC, Bullock JY, Faull RL, Hladky SB, Barrand MA (2010) ABC efflux transporters in brain vasculature of Alzheimer's subjects. Brain Res 1358:228–238
103. Wilhelmus MM, Otte-Holler I, van Triel JJ, Veerhuis R, Maat-Schieman ML, Bu G et al (2007) Lipoprotein receptor-related protein-1 mediates amyloid-beta-mediated cell death of cerebrovascular cells. Am J Pathol 171:1989–1999
104. Wilson RS, Beckett LA, Barnes LL, Schneider JA, Bach J, Evans DA et al (2002) Individual differences in rates of change in cognitive abilities of older persons. Psychol Aging 17:179–193
105. Xue ZQ, He ZW, Yu JJ, Cai Y, Qiu WY, Pan A et al (2015) Non-neuronal and neuronal BACE1 elevation in association with angiopathic and leptomeningeal beta-amyloid deposition in the human brain. BMC Neurol 15:71
106. Xuereb JH, Brayne C, Dufouil C, Gertz H, Wischik C, Harrington C et al (2000) Neuropathological findings in the very old. Results from the first 101 brains of a population-based longitudinal study of dementing disorders. Ann N Y Acad Sci 903:490–496
107. Yamada M (2002) Risk factors for cerebral amyloid angiopathy in the elderly. Ann N Y Acad Sci 977:37–44
108. Yamazaki Y, Kanekiyo T (2017) Blood–brain barrier dysfunction and the pathogenesis of Alzheimer's disease. Int J Mol Sci 18:1965

109. Yousif S, Marie-Claire C, Roux F, Scherrmann JM, Decleves X (2007) Expression of drug transporters at the blood–brain barrier using an optimized isolated rat brain microvessel strategy. Brain Res 1134:1–11
110. Zarow C, Barron E, Chui HC, Perlmutter LS (1997) Vascular basement membrane pathology and Alzheimer's disease. Ann N Y Acad Sci 826:147–160
111. Zenaro E, Piacentino G, Constantin G (2017) The blood–brain barrier in Alzheimer's disease. Neurobiol Dis 107:41–56
112. Zlokovic BV (2005) Neurovascular mechanisms of Alzheimer's neurodegeneration. Trends Neurosci 28:202–208